The role of kinematic events in whisker-related tactile perception

Dissertation

zur Erlangung des Grades eines

Doktors der Naturwissenschaften

der Mathematisch-Naturwissenschaftlichen Fakultät

und

der Medizinischen Fakultät

der Eberhard-Karls-Universität Tübingen

vorgelegt

von

Christian Waiblinger

aus Kusterdingen, Deutschland

November 2014

Tag der mündlichen Prüfung:	06.02.2015
Dekan der Math.-Nat. Fkultät:	Prof. Dr. W. Rosenstiel
Dekan der Medizinischen Fakultät:	Prof. Dr. I. B. Autenrieth
1. Berichterstatter:	Prof. Dr. Cornelius Schwarz
2. Berichterstatter:	Dr. Laura Busse
Prüfungskommission:	Prof. Dr. Cornelius Schwarz
	Prof. Dr. Martin A. Giese
	Prof. Dr. Christoph Braun
	Dr. Laura Busse

Ich erkläre, dass ich die zur Promotion eingereichte Arbeit mit dem Titel:

„The role of kinematic events in whisker-related tactile perception“

selbstständig verfasst, nur die angegebenen Quellen und Hilfsmittel benutzt und wörtlich oder inhaltlich übernommene Stellen als solche gekennzeichnet habe. Ich versichere an Eides statt, dass diese Angaben wahr sind und dass ich nichts verschwiegen habe. Mir ist bekannt, dass die falsche Abgabe einer Versicherung an Eides statt mit Freiheitsstrafe bis zu drei Jahren oder mit Geldstrafe bestraft wird.

Tübingen, den _____ _____

Datum Unterschrift

Table of Contents

1. Introduction **3**

1.1. The rat whisker system 3

1.2. Texture encoding 5

1.3. Aim and scope of this study 7

2. Methods **8**

2.1. Animals, surgery, and general procedures for behavioral testing 8

2.2. Electrophysiology 9

2.3. Whisker Stimulation 10

2.3.1.1. Pulsatile stimuli 11

2.3.1.2. Broadband noise and ‘slip-like’ events 12

2.4. Experimental paradigm 13

2.5. Data analysis and statistics 19

3. Results **22**

3.1. Psychometrics with pulsatile stimuli 22

3.2. Barrel Cortex activity with pulsatile stimuli 31

3.3. Psychometrics with ‘slip-like’ events and background noise 43

4. Discussion **49**

4.1. Support for neuronal coding of instantaneous kinematic cues 49

4.2. Support for the slip hypothesis 52

5. References **55**

Abstract

Rodents use active whisker movements to explore their environment. The physical parameters of vibrissa deflections, which carry the texture information and are used by the tactile system for discrimination, are unknown. Particularly, it remains unclear whether perception relies on parameters such as frequency (e.g., spectral information) and intensity (e.g., mean speed) which need to be integrated over time or whether it has access to instantaneous kinematic parameters (i.e., the details of the trajectory). The search for instantaneous kinematic parameters is motivated by findings from studies on rodent vibrissae biomechanics showing that short-lived kinematic events, abrupt movements called 'slips', carry texture information and could therefore be used for tactile perception. Here, I use a novel detection of change paradigm in head-fixed rats, which presents passive vibrissa stimuli in seamless sequence for discrimination. Unlike previous paradigms, this procedure ensures that processes of decision making do not need to rely on memory functions and can, instead, directly tap into sensory signals. In a first attempt, repetitive pulsatile stimuli were employed in a noise free environment to optimally control the parameter space. I find that discrimination performance based on instantaneous kinematic cues far exceeds the ones provided by frequency and intensity. Neuronal modeling based on barrel cortex single-unit activity shows that small populations of sensitive neurons provide a transient signal that optimally fits the characteristic of the subject's perception. However, a realistic scenario involves background noise (e.g. evoked by rubbing across the texture) and kinematic 'slip' events, carrying texture information. Therefore, if these events are used for tactile perception, the neuronal system would need to differentiate slip-evoked spikes from those evoked by noise. To test the animals under these more realistic conditions, I presented passive whisker-deflections, consisting of 'slip-like' events (waveforms mimicking 'slips' occurring with real textures) embedded into background noise. Varying the event shape (ramp or pulse), kinematics (amplitude, velocity, etc.), and the probability of occurrence, I observed that rats could readily detect 'slip-like' events of different shapes against a noisy background. Psychophysical curves revealed that larger events improved performance while increased probability of occurrence had barely any effect. These results strongly support the notion that encoding of instantaneous 'slip' kinematics dominantly determines whisker-related tactile perception while the computation of time integrated parameters plays a minor role.

1. Introduction

1.1. The rat whisker system

The rodent vibrissae-related tactile system has been studied extensively for about hundred years (Vincent, 1912). With its well defined structural and functional organization, it has been established as an exemplary model system to study neuronal processing underlying perception and sensorimotor interaction. The whiskers are complex tactile organs developed in particular by nocturnal animals living underground that are not able to rely on vision for orientation. Rats and mice use them as tools to sample their spatial environment or detect, localize and discriminate objects (Vincent, 1912; Hutson and Masterton, 1986; Carvell and Simons, 1990; Brecht et al., 1997; Mehta et al., 2007; O'Connor et al., 2010; Stüttgen and Schwarz, 2008; von Heimendahl et al., 2007). Each of the whiskers consists of a stiff modified body hair that is embedded in the skin around the animals' snout in a so-called follicle-sinus complex (Ebara et al., 2002). This complex is innervated by numerous myelinated and non myelinated fibers of the infraorbital nerve, a side branch of the trigeminal nerve. They end either as free nerve endings or specialized mechanoreceptors including merkel cells, lanceolate- and club-shaped endings (Ebara et al., 2002; Rice and Munger, 1986). These diverse innervation types fall into two functional classes, the slowly and the rapidly adapting afferents (SA and RA)(Gibson and Welker, 1983). Arranged are the whiskers in a fixed pattern with the long whiskers ('macro vibrissae'; Brecht et al., 1997) on the side and the short whiskers ('micro vibrissae') on the front of the snout. Due to anatomical advantages (size and easy accessibility) this work focuses exclusively on macro vibrissae. The Macro vibrissae consist of five parallel rows (labeled with A to E from dorsal to ventral) each of which contains four to nine single whiskers (columns, numbered from caudal to rostral). Completed is the whisker pad by the four 'straddlers' (Alpha to Delta) on the caudal end with a downward offset to the rows. The length of the whiskers varies from several centimeters on the caudal end down to a few millimeters on the rostral end close to the lips (Brecht et al., 1997). With intrinsic and extrinsic muscles the whiskers can be moved actively forth and back (Dörfl, 1982; Berg and Kleinfeld, 2003) with a frequency between five and eleven hertz. This behavior during exploration is called 'whisking' (Welker, 1964). Once a whisker touches the surface of an object, it is deflected, due to its biomechanical properties, at an angle

relative to the surface of the skin (Ritt et al., 2008; Wolfe et al., 2008; Pammer et al., 2013). These deflections evoke action potentials in sensory neurons of the trigeminal nerve that excites brainstem trigeminal nuclei (TN). From there sensory information is sent to the ventro-posterior-medial nucleus (VPM) of the thalamus to a second synapse that excites thalamo-cortical projections to the cortex (Figure 1A) (Petersen, 2003, 2007; Feldmeyer et al., 2013). The whisker related representation in primary somatosensory cortex (S1) is remarkably big compared to the rest of the body surface which parallels the overrepresentation of the fingers and face found in primate somatosensory cortex (Penfield and Rasmussen 1950). Arguably the most important characteristic of S1 is its distinct somatotopic organization (Figure 1b). This phenomenon was first discovered by Cajal (Ramon Y Cajal, 1911) and further described by Woolsey and Van der Loos (Woolsey and Van der Loos, 1970). Based on tangential Nissl stained sections, these researchers discovered anatomically distinguishable structures in layer 4 of the primary somatosensory cortex, which were arranged in the same pattern as the whiskers on the skin and according to their shape in frontal sections they were described as 'barrels'. Mapping experiments using microelectrodes (Welker, 1971) confirmed the assumption that the barrel cortex has a precise topographic representation of the whiskers. Neurons of individual barrels respond preferentially to stimulation of the corresponding contralateral whisker (Simons, 1985). This organization can also be found on earlier stages of the ascending pathway, the VPM of the thalamus that contains 'barreloids' relaying mono whisker signals to S1 barrel columns (Lo et al., 1999) and the trigeminal brainstem complex with histologically defined zones termed 'barrelettes' (Jacquin et al., 1990). The thalamo-cortical system is subdivided into a fast, highly resolved, 'lemniscal' system and a slower and more spatially coarse 'paralemniscal' system. The first passes through VPM and terminates predominantly in layer 4 (and to lesser degree in L5B) of the barrel column, whereas the second passes through the posterior-medial (POM) nucleus of the thalamus and terminates mainly in layer 5A but also in layers 4 and 2/3 in strips of dysgranular cortex, called inter-barrel columns. Layer 5 contains huge pyramidal cells integrating inputs from barrel and inter-barrel compartments (Brecht, 2007; Feldmeyer et al., 2013). Although the detailed anatomy is unique to this particular pathway, the functional elements of the circuit are common to other sensory pathways, allowing many aspects of the work proposed here to generalize to both humans and other animal models.

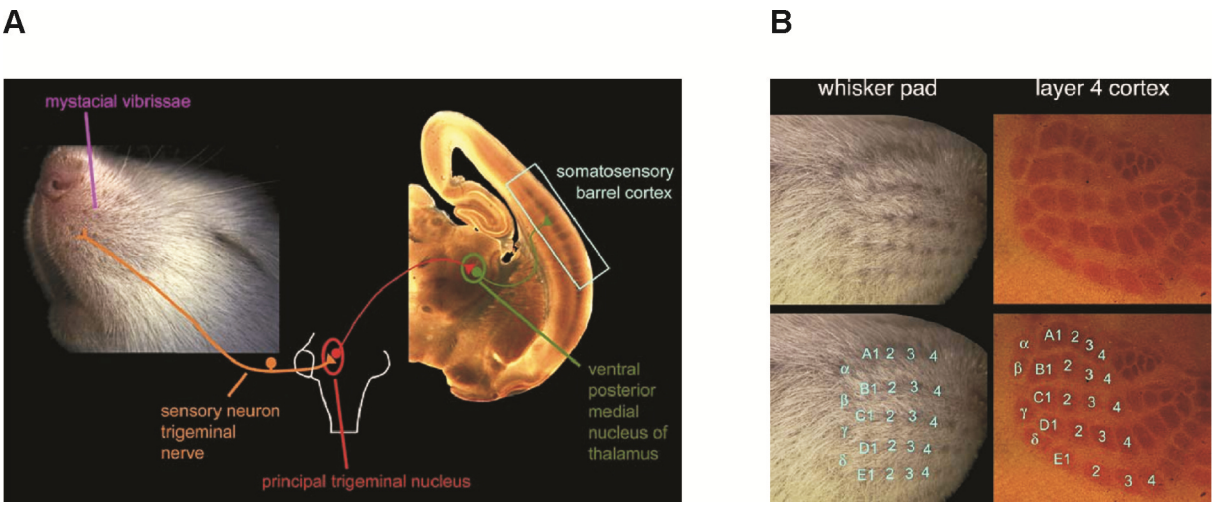

Figure 1. The main features of the rodent whisker system. (A) Ascending pathway from whisker to cortex. Synaptic stations are brainstem, thalamus and barrel cortex. (B) Whisker pad arrangement and tangential section through layer 4 of the primary somatosensory cortex after staining with cytochrom oxidase. Adapted from Petersen (Petersen, 2003).

1.2. Texture encoding

Rodents rub their whiskers across objects to tactilely explore them. Due to biomechanical properties, the whisker vibrations along the hair shaft show a complex and indirect relationship to the textural properties of the object, and finally result in what we call the vibrotactile signal - the movements at the follicle that are directly translated into spike trains of primary afferents. High speed video recordings of moving whiskers revealed so called 'slips' - kinematic signatures contained in the vibrotactile signal, defined by short-lived, fast deflections of the whisker. Under natural conditions slips are based on bioelastic properties of the hair, i.e. its form and elasticity (Hartmann, 2001; Ritt et al., 2008; Hires et al., 2013) but may as well reflect properties of the probed texture (Wolfe et al., 2008; Jadhav et al., 2009), and thus may be used by the animals for tactile perception. The latter conjecture is termed 'slip hypothesis'. In the lab, slips can be mimicked by ‘slip-like’ kinematic signatures (i.e. ramp- or pulse-like whisker deflections), and are applied mechanically directly to the whisker base near the follicle. Different kinematic signatures are represented by highly selective spike responses on the ascending whisker-related tactile system (Jones et al., 2004; Arabzadeh et al., 2005; Petersen et al., 2008; Jadhav et al., 2009; Chagas et al., 2013) and form the major basis for perceptional performance in detection and discrimination of vibrotactile stimuli (Stüttgen and Schwarz, 2010).

The classical parameters 'intensity', and 'frequency', established in work on the primate fingertip system (LaMotte and Mountcastle, 1975), and investigated in similar ways also in the whisker system (Adibi et al., 2012), both carry information about textures (Hipp et al., 2006), but support perception only in suboptimal ways (Stüttgen and Schwarz, 2010). The latter study also revealed that it is unlikely that these classical parameters are encoded in the neuronal signals judging from the fact that neuronal activity can be best fit to behavioral performance when assuming integration time constants of barrel cortex activity in the millisecond range. A recent study that identified intensity as a critical variable (Gerdjikov et al., 2010) also showed that psychometric performance fell short of the one expected if information about instantaneous trajectory characteristics present in individual primary afferents were fully accessible, prompting the question whether the behavioral paradigms used so far have been appropriate to reveal the usage of fully detailed trajectory information. It is possible, that previous task designs entailed process models (i.e., the spatio-temporal description of which brain systems contribute and are critical for performance) that made the read out of instantaneous features impossible or impeded them. For instance, in the Gerdjikov et al. (2010) study, animals had to store vibrotactile information in memory to do the task—discriminanda were presented isolated from each other, such that, in a single trial, the incoming tactile information had to be compared with memory contents. It is intuitive to assume that detailed trajectory information due to capacity limits of the stores cannot be stored in memory, while a time-integrated (i.e., compressed) signal may well offer a less memory-consuming alternative.

1.3. Aim and scope of this study

In the present study, I aimed at improving previous attempts by a behavioral paradigm which allowed subjects to compare discriminanda using purely sensory representations, without memory components, combined with a stimulus set that systematically varies physical parameters and also involves naturalistic whisker 'slips' in a noisy context, mimicking vibrations upon texture contact.

I established a novel task, the 'detection of change' (DOC) psychophysical task, which presents S- (NoGo stimuli predicting no reward) and S+ (Go stimuli predicting reward) in seamless sequence. To compare the discriminanda, subjects do not need to store stimuli in neither working nor long-term memory (Stüttgen et al., 2011). With repetitive pulsatile stimuli, the parameters frequency, intensity, and instantaneous kinematic features can be readily disentangled (Salinas et al. 2000). This enabled me to perform three sets of psychophysical experiments, each of them keeping one of the three parameters (pulse frequency, intensity, and instantaneous kinematic cues) constant during the switch of the stimulus. The experiments were accompanied by extracellular unit recordings in barrel cortex to assess neuronal responses while the animal was engaged in the task thereby enabling a direct correlation between stimulus encoding on the neuronal level and actual behavior. These data have been published recently (Waiblinger et al., 2013).

In order to investigate perceptual skills under more natural conditions I tested rats in two additional behavioral (DOC) experiments with 'slip-like' events of different shape and number, embedded into noisy background vibration of the whisker. This part of the study is in the course of being submitted.

2. Methods

2.1. Animals, surgery, and general procedures for behavioral testing.

All experimental and surgical procedures were carried out in accordance with standards of the Society of Neuroscience and the German Law for the Protection of Animals. Subjects were thirteen female Sprague-Dawley rats (Charles River, Germany), aged twelve to sixteen weeks at the time of implantation. The basic procedures of head-cap surgery, habituation for head-fixation, and behavioral training followed the ones published in a technical review (Schwarz et al., 2010). The animals were anesthetized using ketamine and xylazine (100 and 15 mg/kg body weight, respectively) and chronic electrode arrays (Haiss et al., 2010) were implanted in subjects 1-6. Barrels were located by mapping the cortex with a single intracerebral microelectrode. Unit and field potential responses to a brief manual whisker flick were monitored until a site maximally responsive to flicks of a single whisker with lower activation of adjacent whiskers was found. Across the six animals that were used for electrophysiological recordings, columns A3, C1, C2, D1, and D2 were implanted. Movable multi-electrode arrays were centered over the mapped location and slowly inserted into the cortex at a speed of 1.25 µm s^{-1} until all electrodes had penetrated the dura (usually 300–800 µm). The electrodes were then slowly retracted to a depth of ~250 µm relative to the cortical surface and fixed to the skullcap with dental cement so that the mobility of the array was still guaranteed. The wound was treated with antibiotic ointment and sutured. Analgesia and warmth were provided after surgery. Oral antibiotics (Baytril; Bayer HealthCare, Leverkusen Germany, 2.5% in 100-mL drinking water) were provided for three days before surgery and one week postoperatively. Rats were allowed to recover for at least ten days before habituation training. Groups of three rats were housed together and kept under a 12/12 h inverted light/dark cycle. After complete regeneration, rats were put on a water-controlled diet. Water was given to the animal only when successfully completing a task, such as entering the restrainer box or accepting head-fixation. During testing, water intake was restricted to the apparatus where animals were given the opportunity to earn water to satiety. Testing was paused and water was available ad lib during two days a week. Body weight was monitored daily and typically increased during training. No animal in this study needed supplementary water delivery outside training sessions to keep its weight.

The first step of behavioral training was systematic habituation to head-fixation lasting about two weeks: After the animal was accustomed to the restrainer box, the head screw was hold by hand repeatedly until the animal tolerated fixation for several minutes without signs of stress. Once this level was achieved, the animal was fixated completely to the bracket of the restrainer box and transferred to the training setup. After another week of habituation inside the experimental setup two trainings-/ recording-sessions were usually conducted per day, each lasting for 15-30 min resulting in 100-200 trials depending on the impulsivity and motivation of the animal. During behavioral testing a constant white acoustic background noise (70 dB) was produced by an arbitrary waveform generator (W&R Systems, Vienna, Austria) to mask any sound emission of the whisker stimulators. The main elements of the experimental setup including the head-fixed animal are shown schematically in figure 2A.

2.2. Electrophysiology

For electrophysiological recordings I used movable multielectrode arrays (Haiss et al., 2010). An individual microdrive moved an array of four glass coated tungsten electrodes (Thomas Recording, Giessen, Germany. 2×2; electrode distance, 250-375 µm,). Voltage traces picked up by the electrodes were band-pass-filtered (200-5000 Hz) and recorded at a sampling rate of 20 kHz using a multichannel extracellular amplifier (Multi Channel Systems, Reutlingen, Germany). Spikes from arrays were detected using amplitude thresholds. Two-millisecond cutouts centered on the time bin in which the voltage trace first traversed the amplitude threshold were recorded and sorted offline using a laboratory-written software package (Hermle et al., 2004). Artifacts were removed and neurons sorted to yield either single-unit or multi-unit spike trains. Criteria for classification as a single-unit were conservative and have been described in an earlier study (Möck et al., 2006). Firing rates of all units in the 1 s interval preceding the onset of S+ stimuli were compared between short periods at the start and the end of each behavioral session to clarify whether there were long-term adaptations. Only units in which no statistical significant difference was found between the beginning and end of recording sessions were included in the study to exclude that systematic long-term run down of firing rates played any role for the present results. On average, the firing rate during the first five trials of a session was 6.6 spikes/s (SD = 4.1) compared with 6.3 spikes/s (SD = 3.8) during the last five trials (Student's t-test, P = 0.83, n = 19).

2.3. Whisker Stimulation

Two different whisker stimulators were used in this study, a piezo bender actuator that was identical to the one used by Stüttgen et al. (Stüttgen et al., 2006) for pulsatile stimulation and a galvo-motor (galvanometer optical scanner model 6210H, Cambridge Technology) as described in Chagas et al. (2013) for 'slip-like' and broadband noise stimulation, which required a higher temporal accuracy. Both stimulators were calibrated using a modified phototransistor with a resolution of 20 µs and 1 µm (HLC1395, Honeywell, Morristown, NJ, USA) and an optoelectronic measuring device with a resolution of 1.4 ms and 11 µm (laser emitter and detector; PAS 11 MH; Hama Laboratories, Redwood City, CA, USA) (Stüttgen et al., 2006). To ensure precise whisker deflection, the piezo was equipped with a glass capillary (inner diameter ~300 µm with a narrowed insertion hole as described in Stüttgen et al., 2006). The length of the glass capillary and point of attachment of the piezo element were adjusted such that the ringing of the stimulator was minimal between pulses (<0.1° at frequencies around 1 kHz). The rotor of the galvanometer was equipped with a thin 1 cm long aluminum arm with a small insertion hole at the end (~200-300 µm) for single whisker stimulation. The angular position of the galvo shaft (max. angle: ±26 mechanical degrees) was detected by an optical sensor located in the back of the scanner. The output signal of this sensor was a differential current signal that was fed back to the drive electronics, closing the servo loop, and allowing very fast and accurate stimulation. Amplitudes and velocities were derived from the output signal of the sensor and converted into angular values at the whisker base. Both stimulators contacted the whisker 5 mm (±1 mm tolerance) away from the skin, and thus, directly engaged the proximal whisker shaft, largely overwriting bioelastic whisker properties. The null position of the whisker during pulsatile stimulation and the mean position during broadband noise stimulation was its resting point, with an angle between whisker and skin of about 90°. Stimulation was always delivered in rostro-caudal direction. Voltage commands for the stimulators were programmed in LabVIEW (National Instru-ments, Austin, TX), or Matlab and Simulink (The MathWorks, Natick, Massachusetts, USA).

2.3.1.1. Pulsatile stimuli

Stimuli that were delivered by the piezo element consisted of brief pulsatile deflections (one single pulse corresponding to a single-period sine wave of a 100 Hz frequency; starting from the negative maximum, thus yielding a bell-shaped pulse with smooth on- and offsets; duration 10 ms) presented continuously to one single whisker on the left whisker pad. To manipulate pulsatile stimuli, exclusively two basic parameters, 'interpulse frequency' and 'pulse amplitude', were changed in a trial based fashion. Interpulse frequency is defined as the reciprocal of the interpulse interval, that is, the time elapsed between the onsets of two sequential pulses in seconds. Pulse amplitude is defined by the height of a pulse and is changed by multiplying the signal with a constant. Thus, a change in pulse amplitude leaves the width of the pulse untouched. In fact, pulse-width was fixed at 10 ms in all stimuli used in the present study. Using these two basic parameters, three classical vibrotactile parameters were manipulated: 1) instantaneous kinematic cues, 2) frequency, and 3) intensity. With the pulsatile stimuli used here, numbers 1 and 2 of these correspond simply to the two basic parameters interpulse frequency and pulse amplitude. The last one, intensity, corresponds to mean speed of the stimulus (Gerdjikov et al., 2010), and can be manipulated by both of the basic parameters. It is important to note that a balanced change of the two basic parameters interpulse frequency and pulse amplitude in opposite direction leaves intensity constant while changing frequency and instantaneous kinematic cues, a feat used systematically in the present study. Three different manipulations were carried out to distinguish S+ (rewarded) from S- (nonrewarded) stimuli (Experiments 1a, b, and 2a). The first set of stimuli (used in Experiment 1a) varied frequency, and kinematic variables, but kept intensity constant (balanced change of the two basic parameters in opposite direction). The second set (used in Experiments 1b and 2b) varied intensity and kinematic variables but kept frequency constant (exclusive manipulation of pulse amplitude). Finally, the third set (used in Experiment 2a) varied frequency and intensity, and kept kinematic variables constant (exclusive manipulation of interpulse frequency) (cf. Figure 2). Interpulse intervals ranged from 11.1 to 33.25 ms corresponding to interpulse frequencies of 30-90 Hz (for the stimulus set applied in Experiment 2a, I also tried frequencies down to 10 Hz to improve performance, see Results). These values cover the main frequency range carrying texture information (Hipp et al., 2006). Deflection amplitudes ranged from 3.9 to 11.3° (equivalent

to 0.35-1 mm deflections at 5 mm distance from the whisker base). The chosen frequencies and amplitudes of the pulsatile stimuli used here gave intensities ranging from 482 to 1240°/s (cf. Table 1). The kinematic, frequency, and intensity values were assessed based on the measured trajectory (i.e., the output of the phototransistor tracking the whisker). Using pulsatile stimuli, special care was taken to assure that the change from S- to S+ (and back) occurred within one interpulse-interval, that is, the succession of interpulse-intervals was a clean step function (i.e., no other interpulse interval than the ones defining S- and S+ occurred). Control experiments were conducted by disconnecting the subjects' vibrissa from the stimulator (by retracting it a few millimeters) after the first half of a session, while monitoring of licking was continued. In all animals, task performance broke down after whisker disconnection assuring that the animals were using exclusively tactile cues to perform the task.

2.3.1.2. Broadband noise and 'slip-like' events

Stimuli that were delivered by the galvo-motor consisted of low pass filtered broadband noise sections (Butterworth filter with a cutoff frequency of 100 Hz) of different maximal amplitudes (A_n mean = 0; SD = [0.125, 0.25, 0.5, 1]°) or constant noise of fixed maximal amplitude (SD = 0.5°) applied throughout the entire recording session with unilaterally embedded 'slip-like' features exceeding the noise (A_f = 3, 6, 9 and 12°). In one rat different noise amplitudes (A_n mean = 0; SD = [0.25, 0.5, 1] °) to embed different 'slip-like' features with scaled signal to noise ratios were used (A_f = [(1.5, 3, 4.5, 6), (3, 6, 9, 12), (6, 12, 18, 24)]°). The events consisted either of pulses (single-period sine wave; starting from the negative maximum, thus yielding a bell-shaped pulse with smooth on- and offsets; 100 Hz; duration 10 ms) or ramps (half-period sine wave; starting from the negative maximum, duration 5 ms with a slow decay, half period sine wave; starting from the positive maximum, duration 995 ms). The slowly decaying part of the ramp did not offer an extra cue to the animal (Stüttgen et al., 2006) and was used to reset the stimulator to its null position. To assure a smooth embedding of 'slip-like' events, the noise was silenced (multiplied) with an inverted Gaussian (SD = 10 ms; minimum at the peak is 0, approaching 1 at ± infinity) centered at the time of the pulse peak or the time of the ramp's maximum velocity. As a

result, the fast transitions where smooth and noise free, whereas the slow decay of the ramp was interspersed with noise (Figure 2F). Higher numbers of 'slip-like' features ($N_f > 1$) were presented within a maximal window of 1 s per trial which also represented the time window for response and potential reward. The time window was always initiated by the first event whereas the following events were distributed randomly within the 1 s period with the only constraint that the inter-slip-interval was always larger than 50 ms. Catch trials contained a continuation of the background noise without any embedded features, but the noise silencing used to embed the features was kept to control for its possible function as a cue. In all experiments catch trials were responded with false alarm rates between 0.1 and 0.25. These numbers were similar to the ones measured before in studies using psychophysical detection tasks (Stüttgen et al., 2006; Stüttgen and Schwarz, 2010). Therefore, it could be concluded that the noise silencing episodes by themselves were not perceivable for the rats.

2.4. Experimental paradigm

All thirteen rats were trained on a novel detection of change (DOC) psychophysical task (Figure 2B). In this task, the whisker is continuously vibrated (S-), but vibration parameters change once in a while, an event that is to be detected (S+) and indicated by the animal by licking at a spout to gain a water reward (intertrial interval 4-10 s drawn from a flat probability distribution). Catch trials contained a continuation of S- instead of presenting a S+. In a first step, continuously applied background stimulation was interspersed by a strong stimulus-switch lasting for 1 s automatically followed by the delivery of a water-drop to condition the consummatory response (licking) upon the stimulus-switch. For pulsatile stimuli the switch consisted of a strong change in interpulse-frequency (e.g. 60 Hz), intensity (e.g. 759°/s) or kinematic variables (e.g. 7.17° pulse amplitude). For naturalistic stimulation, mimicking texture induced vibrations, the S- consisted of low pass filtered broadband noise of fixed amplitude (A_n mean = 0°, SD = 0.5°), interspersed by a S+, which contained a strong and rapid succession of 'slip-like' features with amplitudes exceeding the noise (A_f = 12°, N_f = 6-20 pulses, each 10 ms duration, all occurring within a 1 s noise-section). Once the animals regularly licked off the water the task was switched from classical to operant conditioning,

i.e. the reward delivery was made contingent on an operant lick during the occurrence of S+ plus extra 500 ms to allow any temporal integration. Now, the rats were able to retrieve a water reward by licking immediately after they detected the onset of S+. Licking during a 'no-lick-interval' that spanned the last 2 s before the scheduled S+ presentation was punished by resetting time and starting a new inter-trial interval. Psychophysical testing was conducted using the method of constant stimuli which implies the presentation of stimuli in pseudo-random sequence. Pseudo-random order as applied here presented blocks in which all stimuli occurred once in randomly shuffled order (this strategy avoids sessions in which certain types of stimuli are presented toward the end or the beginning of the session by chance). The lick response window (window of opportunity) was now restricted, typically to 1 s (in some sessions 1.5 s) to prevent high false alarm rates during catch trials.

In this study five major experiments were conducted (Figure 2C-F). Experiment 1a presented five intensity-matched pulsatile stimuli, one catch trial, and three additional stimuli that modulated intensity cues. Experiment 1b presented five frequency-matched pulsatile stimuli, one catch trial, and one additional stimulus that modulated frequency cues. Experiment 2a presented five pulsatile stimuli with matched kinematic variables and one catch trial. Experiment 2b was similar to Experiment 1b except it did not contain any additional stimuli; it was simply used as a control experiment. Experiment 3 was exceptional as it consisted of a trial based presentation of 1 s broadband noise sections (S+) of different amplitudes (A_n mean = 0; SD = [0.125, 0.5, 1]°) with no extra background vibration. This control experiment was conducted to test the animals' detection threshold for broadband noise after they had already learned the DOC task. The on- and offset of the noise stimulus was smoothed with a sinusoidal filter (50 ms duration) to avoid abrupt transitions. In experiment 4, the noise stimulus was considered as S- background vibration and applied constantly throughout the entire recording session with a fixed or varying amplitude A_n, whereas the embedded 'slip-like' events (S+) occurred only in a trial based fashion with amplitudes exceeding the noise band. In experiment 4a, 'slip-like' features consisted of single 10 ms pulses embedded in constant broadband noise, whereas in experiment 4b, 'slip-like' features consisted of 5 ms ramps (in both experiments A_n mean = 0; SD = 0.5°; A_f = 3, 6, 9, 12°). Experiment 4c was like experiment 4b, only that here three different blocks of noise amplitudes (A_n mean = 0; SD = [0.25, 0.5, 1]°) and three blocks of adjusted ramp amplitudes

were presented (A_f = [(1.5, 3, 4.5, 6), (3, 6, 9, 12), (6, 12, 18, 24)]°). Between the three different conditions the signal to noise ratio (A_f/A_n) was kept constant. To avoid confusing the animal by abruptly changing the noise amplitude, the different noise conditions were presented in separate sessions. Finally, in experiment 5 the numbers of 'slip-like' features (N_f) and the amplitudes (A_f) exceeding the noise band were varied, resulting in thirteen possible stimuli including catch trial (A_n mean = 0; SD = 0.5 °; A_f = 3, 6, 9, 12°, N_f = 1, 3, 6). Animals 1-6 were used in experiment 1-2 (table 1), whereas animals 7-13 were used in experiment 3-5 (table 2).

Figure 2. Setup and experimental strategy. (A) Schematic of a head-fixed rat inside the restrainer with water spout, whisker stimulator and chronically implanted electrodes. (B) Subjects were trained on a detection of change (DOC) task. Constant stimuli were applied to a single whisker and the animals had to detect a 1 s change (S+, gray box) with a lick response in order to get a water reward. No change served as catch trial (S-). Impulsive licks triggered extra time of background stimulation. (C) Overview of pulsatile stimuli applied in experiment 1 and 2 (first column). The general idea was to keep one of the three vibrotactile parameters intensity (I, experiment 1a), frequency (F, experiment 1b), or instantaneous kinematic cues (K, experiment 2a) constant between S- and S+ (second column) and only vary the other two. Schematic stimulus waveforms at the time of stimulus transitions are shown in the fourth column. Using pulsatile stimuli, an increase of instantaneous kinematic cues (i.e., increase of pulse amplitude) is correlated with intensity but not pulse frequency. (D) In Experiment 2a, the instantaneous kinematic cues are constant; therefore, the observer has to integrate the running stimulus with a minimal time window comprising more than one pulse (>10 ms). Stimulus transitions filtered with integration windows of different size (red boxes = moving average) demonstrate that perfect discrimination of these stimuli can theoretically be performed very soon after stimulus onset. (E) Overview of noise stimuli applied in experiment 3-5. In experiment 3, perceptibility of broadband noise was assessed by presenting 1 s sections of different noise-levels (A_n). In all the following experiments the noise served as background (S-) and was presented continuously throughout the entire session. In experiment 4 'slip-like' features (S+) of different amplitudes (A_f) and shapes (pulses in experiment 4a or ramps in experiment 4b) were embedded exceeding the kinematics of the noise band. The noise amplitude (A_n) was additionally varied in experiment 4c. In experiment 5 'slip-like' features of different amplitudes (A_f) and numbers (N_f) were embedded. (F) Examples of pulse-shaped or ramp-shaped 'slip-like' features of different amplitudes embedded into broadband noise of constant amplitude (n = 100 trials overlaid in each panel). The noise was silenced with an inverse Gaussian at the time of feature location, thereby smoothing the fast transitions.

A

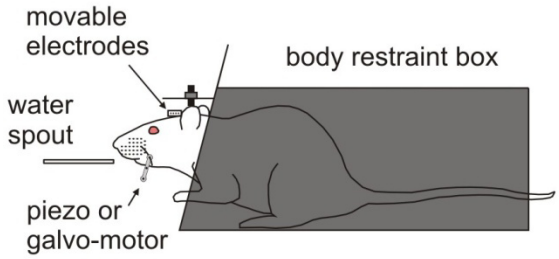

B

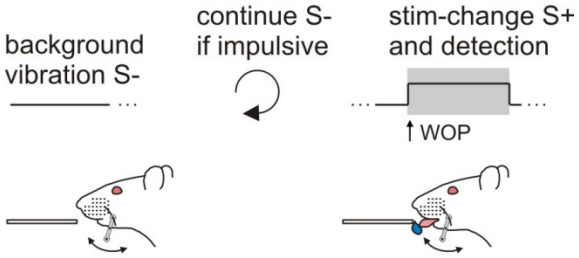

C

exper-iment	constant parameter	change S+	example (S- S+)
1a	**I**	**A & F**	
1b	**F**	**A & I**	
2a	**K**	**F& I**	
2b	**F**	**A & I**	

D

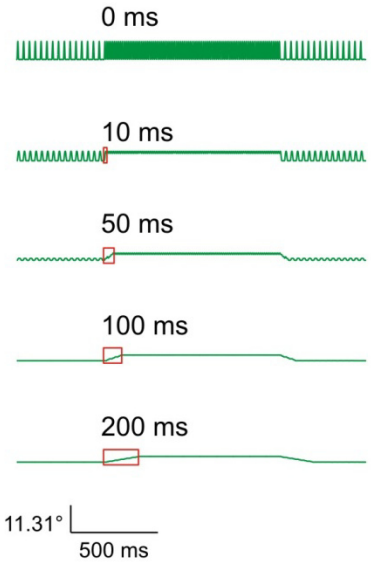

E

exper-iment	**back-ground S-**	**change S+**	**example (S- S+)**
3		**noise with varying A_n**	
4a	**noise with fixed A_n**	**pulse with varying A_f**	
4b	**noise with fixed A_n**	**ramp with varying A_f**	
4c	**noise with varying A_n**	**ramp with varying A_f**	
5	**noise with fixed A_n**	**pulse with varying A_f and N_f**	

F

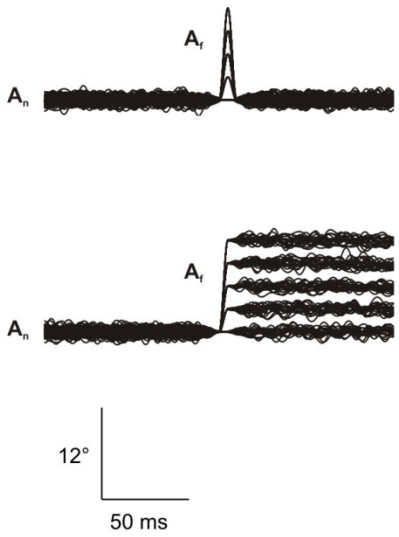

Table 1. Pulsatile stimuli and psychophysical experiments.

		Intensity (°/s)	Frequency (Hz)	Amplitude (°)	N-Trials		
					Rat 1	2	3
Experiment 1a	S_-	646	90	4.14	536	605	617
	S_+ - S_-	0	-12	+0.33	586	596	616
		0	-24	+1.14	586	649	553
		0	-36	+2.20	579	609	642
		0	-48	+3.86	567	631	648
		0	-60	+7.17	576	615	624
	S_+ - S_-	+64	-24	+1.66	366	425	471
		-64	-24	+0.62	424	507	444
		-128	-24	+0.09	452	513	455
Experiment 1b	S_-	507	66	4.14	626	489	454
	S_+ - S_-	+41	0	+0.33	637	502	461
		+140	0	+1.14	636	509	447
		+268	0	+2.20	567	525	468
		+464	0	+3.86	676	531	471
		+844	0	+7.17	630	475	513
	S_+ - S_-	+140	+24	0	630	508	445
					Rat 4	**5**	**6**
Experiment 2a	S_-	1240*	90*	7.76	272	136	49
	S_+ - S_-	-131*	-12*	0	303	190	69
		-291*	-24*	0	316	159	51
		-451*	-36*	0	287	159	63
		-602*	-48*	0	282	184	70
		-759*	-60*	0	314	193	49
Experiment 2b	S-	482	66	3.90	319	271	302
	S_+ - S_-	+157	0	+1.29	299	252	297
		+307	0	+2.53	305	251	317
		+468	0	+3.85	363	295	297
		+628	0	+5.17	366	283	298
		+759	0	+6.34	345	244	304

* in rat 5 stimulus order was reversed: the absolute intensity and frequency of S_- was 482 °/s and 30 Hz respectively, the difference S_+ - S_- was in this case always positive (same value).
Data in light gray fields describe added stimuli that deliberately varied the parameter that was else kept constant in the respective experiment (cf. Figure 3CD).

Table 2. Broadband noise with 'slip-like' stimuli and psychophysical experiments.

Experiment	Stim-type	A_n 2SD (°)	A_f (°)	N_f	N-Trials						
					Rat 7	8	9	10	11	12	13
3	S-	0	0	0	156	228					
	S+ noise	0.25	0	0	156	230					
		0.5	0	0	154	230					
		1	0	0	155	229					
		2	0	0	156	230					
4a	S-	1	0	0	226		132	165	174		
	S+ pulse	1	3	1	225		132	165	174		
		1	6	1	225		130	165	175		
		1	9	1	225		131	167	175		
		1	12	1	226		134	167	175		
4b	S-	1	0	1	200	267				175	151
	S+ ramp	1	3	1	199	265				175	152
		1	6	1	196	268				175	148
		1	9	1	199	266				174	150
		1	12	1	198	265				172	151
4c	S-	0.5	0	0	203						
		1	0	0	200						
		2	0	0	201						
	S+ ramp	0.5	1.5 3 4.5 6	0	201*						
		1	3 6 9 12	0	196*						
		2	6 12 18 24	0	200*						
5	S-	1	0	0		157	161	106	148		
	S+ pulse	1	3	1 3 6		155*	160*	105*	147*		
		1	6	1 3 6		157*	159*	106*	145*		
		1	9	1 3 6		156*	161*	106*	149*		
		1	12	1 3 6		158*	162*	107*	145*		

* The numbers correspond to the minimum values.

A_n = Noise Amplitude

A_f = Feature Amplitude ('slip-like' event)

N_f = Numbers of feature ('slip-like' event)

2.5. Data analysis and statistics

Psychophysical data was assessed as mean response-probabilities across trials and sessions during presentation of S+ stimuli and catch trials (S-). The psychometric curves in this study are Weibull or Logistic fits estimated from a maximum likelihood estimator (Wichmann and Hill, 2001a, b). Error bars of psychometric data signify 95% confidence intervals calculated from a binomial model setting the animal's response probability to the probability of a Bernoulli trial. Statistical differences between psychophysical data was assessed using 95% confidence limits of the thresholds (probability of detection = 0.5). Response probabilities were converted into sensitivity d' using the following equation:

$$d' = \Phi^{-1} p_{hit} - \Phi^{-1} p_{FA} \quad (1)$$

where p_{hit} signifies the probability of correct responses, p_{FA} the probability of false alarms, and Φ^{-1} is the probit function. In order to compare psychometric with neurometric sensitivities, d' values were converted to area under the receiver operating curve (AUROC) (Stanislaw and Todorov, 1999) by

$$AUROC = \Phi(\frac{d'}{\sqrt{2}}) \quad (2)$$

(for the correction term $\sqrt{2}$ see ref. Stüttgen et al., 2011); note that despite the typing error in their equation (3), this is identical to what has been done by Gerdjikov et al. (2010). To give a rough estimate of psychophysical performance across sessions of experiments 1 and 2 (Figures 3B and 4B), a simple discrimination index was calculated

$$di = p(r|S+) - p(r|S-), \quad (3)$$

where $p(r|S+)$ is the response probability to presentation of the strongest S+ and $p(r|S-)$ is the response probability to S-.

Reaction times of experiment 4-5 were calculated by subtracting the timestamp of the first lick within the 1 s window of opportunity from the onset of the respective 'slip-like' event.

Neuronal sensitivities were computed from distributions of cortical spike counts calculated as the difference of the spike counts found in intervals of equal length just before and after each onset of pulsatile stimulus change (negative spike counts indicate a suppressed response under S+ relative to background). A criterion shifted in steps of one spike across the two distributions was used to determine the hits and false alarms of the neuron, and thus the ROC curves (Britten et al., 1992). Sensitivities for all S+ are expressed as AUROC. Neurometric sensitivities of pools of neurons were fitted to the psychometric one by applying a Monte Carlo maximum likelihood procedure (Stüttgen and Schwarz, 2008). The database included the probability of spike counts in a varying window after stimulus onset (as calculated from 50 single-unit trains recorded in Experiment 1a and 24 single-unit trains recorded in Experiment 1b). The fit was performed for all combinations of four parameters: 1) the number of most sensitive neurons accepted into the pool (3, 5, 10, and 15), 2) the pool size (5, 10, 20, 40, 100, 200, and 500), 3) the duration of the time window in which spikes were counted (12.5, 25, 50, 100, 200, 400, and 800 ms), and 4) the prior expectation of the animal of receiving a stimulus that predicts reward, that is, the probability of the occurrence or absence of a certain stimulus according to the subject's knowledge about stimulus ratios. This prior ratio was varied between the extremes PR_{min} = 1/8 (number of catch trials divided by the number of S+ in Experiment 1a) and PR_{max} = 10/5 (time of background stimulation divided by the time of S+ presentation, average from all sessions that entered the dataset). To reliably account for neuronal responses despite the limited number of spikes that could be sampled in the course of one session, I focused exclusively on spike counts (thus ignoring information potentially included in temporal spike patterns, cf. Stüttgen and Schwarz, 2008). In each resampling step, the selection of pool units was performed by a random pick (with return) from a subset of neurons taken from the top of a ranked list according to their sensitivity (assessed from responses to S+ with a maximum of 7.2° amplitude difference to the background stimulus using equation 2). Based on the measured response probabilities, the responses of each pool member to all stimuli were determined by a random pick. These resulted in the likelihood function of each neuron. Assuming independence of neuronal responses, the pool's response was then found by summing the logarithmized likelihood functions of all pool members. The decision was formed by comparing the likelihoods for each stimulus (S+) versus no stimulus (S −). From

Bayes' rule, one can derive that it is optimal to decide for hypothesis h1 versus the alternative h2 if

$$\mathrm{LR}_{1,2} = \frac{\mathrm{l}(\mathrm{h}_1|\mathrm{r})}{\mathrm{l}(\mathrm{h}_2|\mathrm{r})} = \frac{\mathrm{p}(\mathrm{r}|\mathrm{h}_1)}{\mathrm{p}(\mathrm{r}|\mathrm{h}_2} > \frac{\mathrm{p}(\mathrm{h}_2)}{\mathrm{p}(\mathrm{h}_1)} = \mathrm{PR}_{2,1} \quad (4)$$

that is, if the likelihood ratio of h_1 and h_2 given the pool response r ($LR_{1,2}$) exceeds the inverse ratio of the respective prior probabilities $PR_{2,1}$. The optimal criterion (converted to log space) to decide about the presence of a stimulus then is

$$\log\big(\mathrm{p}(\mathrm{r}|\mathrm{s}_\mathrm{i})\big) - \log\big(\mathrm{PR}_{2,1}\big) > \log\big(\mathrm{p}(\mathrm{r}|\mathrm{s}_{\mathrm{catch}})\big). \quad (5)$$

On the left side of the inequality, $PR_{2,1}$ is accounted for by taking the logarithm and subtracting from the log likelihood of the stimulus (s_i). The right side holds the log likelihood of the catch trial given r. The pool's decision was set to 1 (stimulus present) if any comparison favored the presence of a S+ (i. e. equation 5 was true), otherwise it was set to 0 (i. e. equation 5 was false). The pool's neurometric responses were calculated based on its decisions exactly as done with the behavioral data gained from the rat (see above), and compared with psychometric response curves using the Euclidean distance.

3. Results

3.1. Psychometrics with pulsatile stimuli

The first set of psychophysical data (experiment 1-2) was sampled from two groups of three rats each subjected to a DOC paradigm (Figure 2B). Pulsatile stimulation was applied to the base of one whisker (5 mm from the base) with a piezo bender. All animals learned the DOC task after they underwent the training steps described above. I tested whether rats used one of three vibrotactile stimulus parameters for discrimination: 1) 'instantaneous kinematic cues' which can be used to detect so called kinematic events, or extremes in amplitude or velocity, 2) 'pulse frequency,' and 3) 'intensity' as measured by mean speed in an interval minimally encompassing one stimulus period (interval between two sequential pulse onsets). The choice to measure intensity as mean speed was based on psychophysical results showing that rats confound stimuli matched in mean speed (Gerdjikov et al., 2010). To change instantaneous kinematic cues, pulses were multiplied with a constant factor resulting in pulses with different amplitudes and maximal velocities. Changes in frequency were introduced by manipulating interpulse intervals. By applying one of these two manipulations, instantaneous kinematic cues and frequency can be changed independently. However, the intensity of the stimulus is duly affected by both manipulations. Therefore, to keep intensity constant, the pulse amplitude and the interpulse interval had to be changed in reverse directions. Three sets of changes from S- to S+ could be constructed by manipulating pulse amplitude and interpulse interval in a systematic way, each keeping one of the vibrotactile stimulus parameters constant while changing the other two (Figure 2C). This strategy is not possible with the classically applied sinusoid waveforms where changes in frequency necessarily cause changes in both the remaining parameters as well. Experiment 1, performed with the first group of rats, was designed to test the contribution of instantaneous kinematic cues, and therefore, held first the intensity (Experiment 1a) and then the frequency (Experiment 1b) constant between S- and S+, while the pulse amplitudes changed. Experiment 2a then tested if rats temporally integrate the stimulus to extract frequency or intensity information from stimuli that did not offer any differences in pulse waveforms (i.e., kinematic events that could be extracted were identical). I wish to stress that for Experiment 2, a second group of naïve rats were used (rather than testing the animals that already learned the tasks in Experiment 1). This was done to exclude the

possibility that subjects may have learned an inappropriate strategy due to their prior experience (in Experiment 1) with stimuli that differed in amplitude. This strategy assured that in case of minor performance on the task of Experiment 2a, one can exclude the possibility that rats did not perform well because their learning ability was impaired by whatever they had learned before. In order to investigate how the temporal evolution of such an integration compares to the duration of stimuli, running averages of stimulus transitions were computed from windows of different lengths (10–200 ms) and are shown for one stimulus used in Experiment 2a (Figure 2D). Assuming an optimal discriminator, minimal integration time needed to discriminate the stimuli is one period (33 ms for pulsatile stimuli at the lowest frequency of 30 Hz). Although one does not know the properties of the hypothesized integrator, with this analysis, one can be fairly confident that the integration time needed to discriminate stimuli is going to be a small fraction of a second, very likely below 100 ms, which will give the rat ample time to respond during stimulus duration (typically 1 s, some sessions of Experiment 2a used 1.5 s).

Experiment 1a used stimuli that displayed constant intensity, which could be detected either by monitoring instantaneous kinematic cues or by integrating the signal for frequency decomposition. Previous results using a standard trial-based Go/NoGo psychophysical task without background stimulation and similar stimuli, predicted that the animals should have difficulties to discriminate these stimuli, as intensity has been found to be the decisive cue in the earlier task (Gerdjikov et al., 2010). In contrast to this expectation, all three rats of this group working on the DOC paradigm could readily discriminate the stimuli, indicating intensity coding is not necessary in the present context (Figure 3A, red psychometric curves). Experiment 1b used the same amplitude differences between S- and S+ but the pulse frequency of 66 Hz was kept constant. Switched to the new stimulus set, the animals immediately performed well (Figure 3A, blue psychometric curves). Within the first session their response was nearly as good as with the old stimulus set (Figure 3B). The presentations of stimulus sets 1a and b were then alternated in blocks of 10 sessions, and performance never dropped when switching between experimental blocks. Consequently, the psychophysical curves shown in Figure 3A have been constructed from all sessions including the ones right after switching from one stimulus set to the next. Plotted across instantaneous kinematic cues (the shared parameter between stimulus sets 1a and b), the

two psychometric curves are nearly identical for all three rats (blue and red curves in Figure 3A). The confidence limits of the two curves overlap for all stimuli except for a slight deviation of the response to stimuli at amplitude difference 1.1° in rat 1. This demonstrates that stimuli lacking either intensity or frequency cues are detected equally well, suggesting that instantaneous kinematic features are the relevant cue used by the animals during discrimination. This conclusion is supported further by the analysis of additional stimuli that were presented together with the core stimulus sets in Experiments 1a and b reported so far. These additional stimuli (randomly inserted into the sequence of core stimuli) deviated from the equal intensity (1a), or frequency (1b) rule respectively. I asked whether discrimination would improve if some intensity cue (1a) or frequency cue (1b) were added to a stimulus close to perceptual threshold (1.1° amplitude difference). Experiment 1a contained three additional stimuli, two deviating downward and one deviating upward from the intensity of the original 1.1° stimulus (see schematic in Figure 3C). This was done by manipulating the pulse amplitude of the stimulus; thus, it was a co-manipulation of intensity and instantaneous kinematic cues. In the downward direction, the intensity cue decreased (because it deviated more and more from that of the S-) but, at the same time, the amplitude was drawn closer to the one of S-, in fact reducing the instantaneous kinematic cue. The expectation then was that the animals should show better discrimination whenever they used the intensity cue while they should show the opposite if they used instantaneous kinematic cues. Clearly, in all animals, the latter was the case supporting the hypothesis that they used dominantly instantaneous kinematic cues to solve the task (Figure 3C). Note that the performance of all rats on stimuli with negligible amplitude differences (-128°/s in Figure 3C, +24 Hz in Figure 3D; significantly so in rats 1 and 2) was small but better than catch performance (black outlined box). This indicates the remaining ability to discriminate stimuli after abolishing all instantaneous kinematic cues. In Experiment 1b, one stimulus of increased frequency was added while reducing the pulse amplitude to match the intensity of the original stimulus (see schematic in Figure 3D). The same logic applies here. The animals should discriminate this stimulus better if they used the introduced frequency cue but they should perform worse if they used the abolished instantaneous kinematic cue. Again, the latter was clearly the case in all animals (Figure 3D).

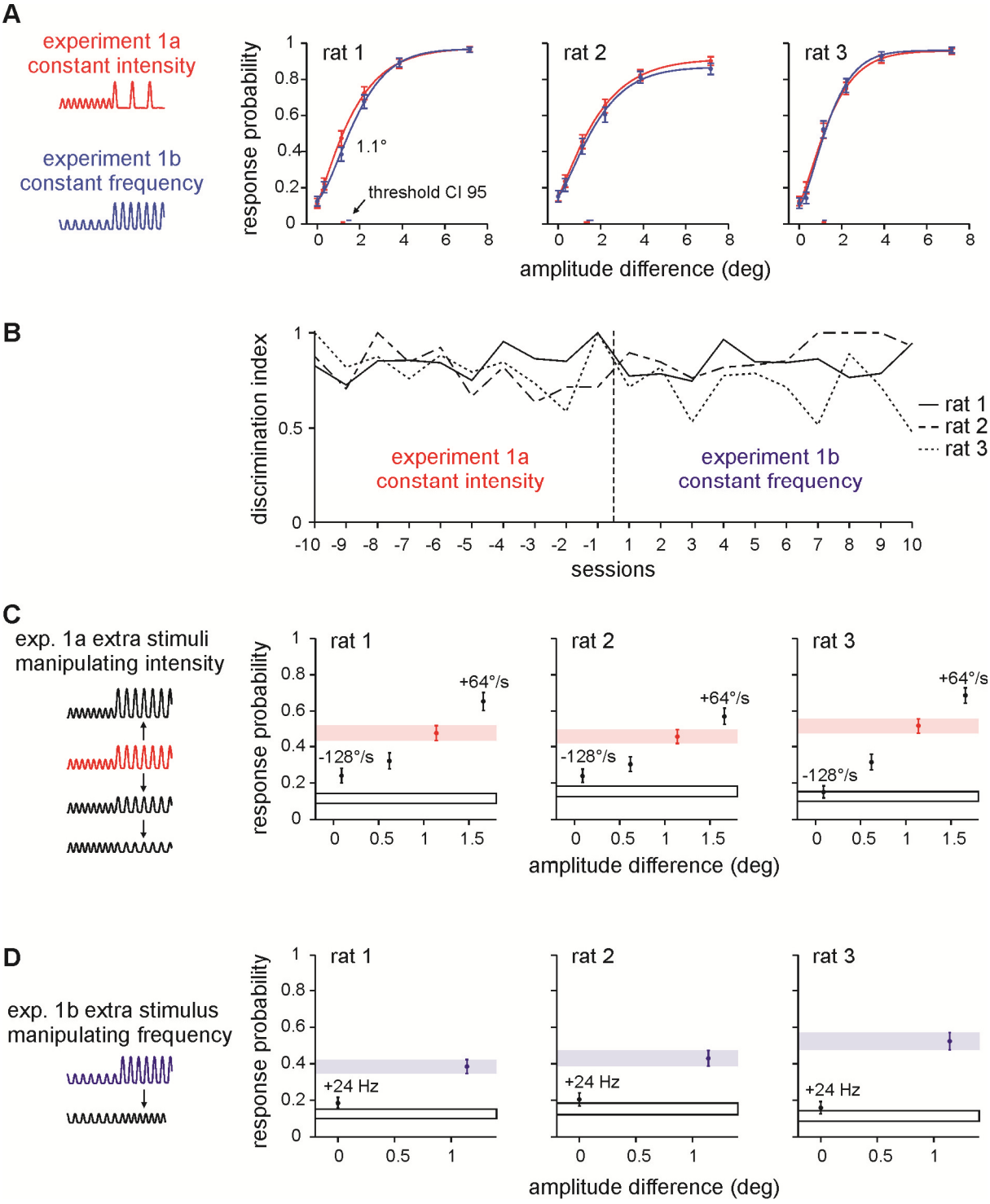
A
experiment 1a
constant intensity
experiment 1b
constant frequency
response probability
rat 1
rat 2
rat 3
1.1°
threshold CI 95
amplitude difference (deg)
B
discrimination index
experiment 1a
constant intensity
experiment 1b
constant frequency
rat 1
rat 2
rat 3
sessions
C
exp. 1a extra stimuli
manipulating intensity
response probability
rat 1
rat 2
rat 3
+64°/s
-128°/s
amplitude difference (deg)
D
exp. 1b extra stimulus
manipulating frequency
response probability
rat 1
rat 2
rat 3
+24 Hz
amplitude difference (deg)

Figure 3. Psychometric performance with two stimulus sets that both employed kinematics as discriminative cues. (A) Response probabilities of three rats are depicted as a function of amplitude differences in red for Experiment 1a and in blue for Experiment 1b. Data points represent means and are based on 447-676 trials. Smooth lines are Weibull fits estimated from a maximum likelihood estimator. Vertical error bars represent 95% confidence intervals. Horizontal bars at the bottom represent 95% confidence intervals of the thresholds. (B) Discrimination index (equation 3) achieved in the last 10 sessions of the first block of Experiment 1a and the first 10 sessions after switching to Experiment 1b. (C) Additional stimuli with manipulated intensities were introduced to test the animals' sensitivity compared with a stimulus with matched intensity from the psychometric curve (colored bar). (D) Same as in C but additional stimuli that modulated frequency. Performance to catch trials is shown as black outlined box. Schematics of stimulus traces used in each experiment are shown on the left side.

The results presented so far strongly argue in favor of the hypothesis that the animals used mainly instantaneous kinematic cues of the pulses as the cue to perform discrimination. Regarding our previous study (Gerdjikov et al., 2010), this fits the hypothesis that the preference for intensity only emerges if instantaneous kinematic features are not available as discriminant cue. However, it is also possible that in principle rats can use all parameters of vibrotactile stimuli to perform discrimination, but they stick to the cue presented when learning the task for the first time and refuse (or are unable) to relearn if the cues change later on. Particularly, I was concerned that in Experiments 1a and b, the animals adopted the strategy to watch out for the first different pulse (with respect to the background S- pulses) to perform the task. Such a strategy could possibly divert them away from integrating the stimulus (and the use of intensity or frequency cues). In order to address this point, I designed an experiment to investigate how a second set of naïve rats learned the task if instantaneous kinematic cues (i.e., a divergent waveform or 'oddball' pulse) were absent from the start. Experiment 2a held instantaneous kinematic cues (i.e., the pulse waveform) constant across stimuli and thus forced the subjects to use temporal integration, if they could. Later, a stimulus set very similar to the one in Experiment 1b was presented in Experiment 2b, to check if the animals would switch to instantaneous kinematic cues when present or stay with whatever they learned in Experiment 2a (Figures 2C and 4A).

The hypothesis that animals learn the task equally well using any of the three parameters was rejected by Experiment 2a. A second naïve set of three rats showed great difficulties learning the task when instantaneous kinematic cues were absent (Figure 4A, green curves). An extension of S+ duration to 1.5 s and the use of larger frequency differences, 90 versus 10 Hz (data not shown) in some training sessions did not help. The resulting psychometric curves indicated hit rates between 0.45 and 0.71 during presentation of the strongest stimulus change and false alarm rates between 0.29 and 0.43 during catch trials (with n = 49-316 trials per stimulus). Rat 5 experienced positive changes in intensity (intensity S-< intensity S+) while rats 4 and 6 were confronted with negative changes (intensity S-> intensity S+; see Table 1 for details). Only rat 4 was able to perform reasonably well (hit rate 0.71, false alarm rate = 0.29), but never reached the performance achieved by the first set of animals that experienced changes in kinematic cues. Moreover, rat 6 refused to work on the task at one point, forcing me to terminate this part of the experiment at a lower number of sampled trials than intended (cf. Table 1). Finally, when I switched to a stimulus set that

contained instantaneous kinematic cues (but held frequency constant, Experiment 2b) all three rats readily learned the task (Figure 4A, blue curves). The transition of the general discrimination index after the first switch to Experiment 2b is shown in Figure 4B. After learning to discriminate stimulus set 2b, the rats were repeatedly switched back to Experiment 2a but never showed any improvement in discrimination performance on this stimulus set. As shown in Figure 4C, the performance of the successful rat 4 was roughly in the range of performances observed using a quite different psychophysical design but similar stimuli (no instantaneous kinematic cues) (Gerdjikov et al., 2010). I wish to stress that this comparison must be viewed with caution— not only because the data were obtained with different psychometric paradigms—but also because, in the previous study, the S+ were the higher frequency stimuli while the present rat 4 was confronted with S+ that were of lower frequency than S-. Nevertheless, I find the comparison instructive as it shows that the exclusive presence of intensity and frequency cues does not abolish discrimination performance but rather is able to grant a minor amount of discrimination ability consistent with the previous results using a quite different task design. In summary, these experiments conclusively show that the usage of a certain type of cue is not dependent on the sequence of learning. Furthermore, they show that it is also not due to a bias generated by the structure of the psychophysical Experiment 1ab, which potentially led the animals' to use the strategy to detect oddball pulses. Rather, the results point to a limitation of perceptual capabilities of the rats: they show superior performance when instantaneous kinematic cues are present, and their ability to discriminate vibrotactile stimuli using frequency or intensity cues is minor.

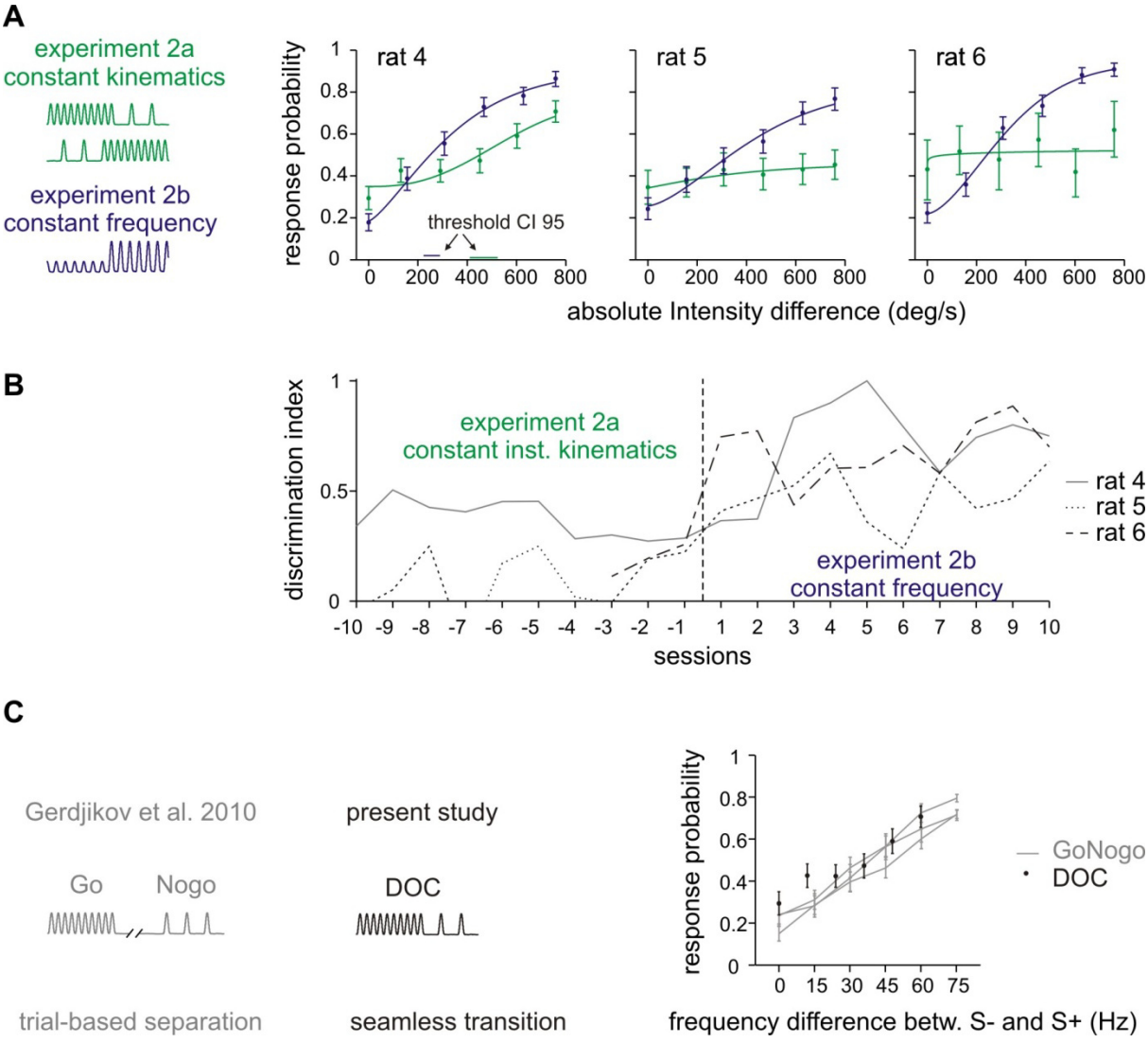
A
experiment 2a
constant kinematics
experiment 2b
constant frequency
rat 4
rat 5
rat 6
response probability
threshold CI 95
absolute Intensity difference (deg/s)
B
discrimination index
experiment 2a
constant inst. kinematics
experiment 2b
constant frequency
rat 4
rat 5
rat 6
sessions
C
Gerdjikov et al. 2010
present study
Go
Nogo
DOC
trial-based separation
seamless transition
response probability
GoNogo
DOC
frequency difference betw. S- and S+ (Hz)

*Figure 4. Psychometric performance without kinematic cues. (*A*) Response probabilities of three rats are depicted as a function of intensity differences in green for Experiment 2a and in blue for Experiment 2b. Data points represent means and are based on 49-316 trials. Weibull fits and statistics are the same as in Figure 3. 95% confidence intervals of the thresholds (horizontal bars) are only shown if the psychometric curve surpasses the threshold. Rats 4 and 6 experienced negative change (intensity and frequency of S+ was lower than that of S-, upper green icon), rat 5 worked on the inverted stimulus relationship (intensity/frequency S+ >intensity/frequency S-, lower green icon, see details in Table 1). Rats were naïve before being trained on stimulus set 2a. (*B*) Discrimination index (equation 3) achieved in the last ten sessions of the first block of Experiment 2a (no kinematic cue) and the first ten sessions after switching to Experiment 2b (almost identical to 1b, see Table 1). Note that the index in sessions 1-7 before switching to 2b was not plotted for rat 6. This individual was frustrated by stimulus set 2a and thus was presented only with extreme stimuli (S- and strongest S+) in these sessions in an attempt to keep up its motivation. (*C*) Comparison of psychometric results with an earlier study using the same type of stimuli* (Gerdjikov et al., 2010)*. The earlier study (left) used a classical Go/NoGo paradigm with stimuli separated in time; S+ was the highest frequency stimulus (90 Hz). The present study used a DOC paradigm with seamless presentation of S- and S+ (center). The psychophysical results of rat 4 (the one successfully trained on the DOC task) was obtained with S- being the highest frequency stimulus (90 Hz). Despite the differences in psychophysical design and in stimulus-reward association, the psychophysical results of the two experiments are comparable (right). To allow direct comparison of the curves, the absolute stimulus frequencies used in the earlier study, were converted into frequency differences between S+ and S-.*

3.2. Barrel Cortex activity with pulsatile stimuli

Barrel cortex activity has been shown to be critical for whisker-based passive detection and discrimination (Miyashita and Feldman, 2013). I, therefore, investigated how barrel cortex unit activity represents the present stimuli and explored possibilities for perceptional read-out. During the behavioral session of rats 1-3 (Experiment 1), I recorded a total of 74 single-units and 91 multi-units (Experiment 1a: 50 SU, 61 MU; Experiment 1b: 24 SU, 30 MU) in the barrel column associated with the stimulated whisker. By gradually moving the electrodes, neurons were found between 400 and 1700 µm. Figure 5 shows representative neuronal responses to different S+ and catch trial (the threeunits shown were recorded in the same session of Experiment 1b). All units generated a phasic response in response to the first few pulses after a stimulus switch (best seen with the highest amplitude difference). This pattern is indicative of cortical (re-) adaptation with fairly short time constants kicking in after the stimulus switch. Similar observations have been made with pulsatile stimuli engaging the cortex in the nonadapted (idle) state (Stüttgen and Schwarz, 2010). After the transient response at S+ onset, the firing rate settled at a new level for the remainder of the S+ presentation. With respect to S-, this sustained firing during S+ was elevated in part of the cells (Figure 5, bottom), and it was reduced in very few (Figure 5, top). In many cases, however, sustained firing rate appeared the same in both conditions, and the only visible signs of S+ presence were the transient ON and OFF responses (Figure 5, center).

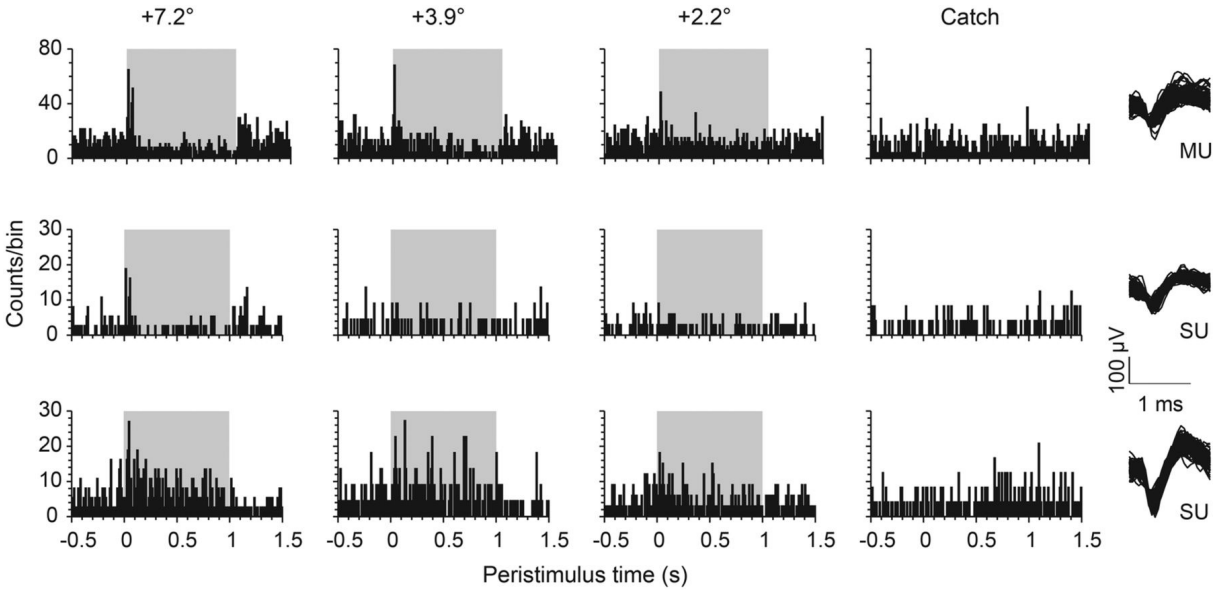

Figure 5. Example cortical responses to changes in pulsatile stimuli (Experiment 1b). PSTHs of representative barrel cortex units recorded from one animal in one session of Experiment 1b. Spike counts across time (bin width 10 ms) are plotted for two single-units (SU) and one multi-unit (MU) (the right column plots a random selection of 100 waveforms for each unit). The other columns plot the response to three different S+ amplitudes (label indicates the difference of S+ and S- pulse amplitudes) and catch trials. The gray area represents the time of stimulus change (S+).

In Figure 6A the distribution of PSTHs obtained from the whole sample are shown for four different stimuli and catch trial used in Experiment 1b. Median firing rate changes (black) and 25% and 75% percentile levels (yellow and green) are depicted for the 30 multi-units (top) and 24 single-units (bottom) recorded in this experiment. The sustained firing rate to S- was subtracted, so that positive/negative firing rates would indicate a higher/lower sustained response to S+ as compared with S-. The median firing rate of multi-units was clearly modulated by the first pulses with amplitude changes down to +2.2°. Inspection of different percentile levels reveals that more than 75% of the multi-units showed an excitatory response to amplitude changes of 7.2° and 3.9°. Owing to very low firing rates, single-unit population activity appeared noisier but generally matched the observation from multi-units. Interestingly, in experiments which kept pulse kinematics constant but varied frequency (labeled '+24 Hz'), all recorded neurons showed flat PSTHs varying around zero change in firing rate. This result reveals the near complete absence of neuronal responses to an isolated switch in stimulus frequency. Nevertheless, as mentioned above, rats display the low but consistent ability to discriminate even when instantaneous kinematic cues were absent (cf. Figures 3C, D and 4C). To examine more closely the sustained firing rates that might give to rise this accomplishment, I compared the firing rate response shortly after stimulus onset, at the end of stimulus presentation, and for the entire stimulus period for the total sample of single- (n = 74) and multi-units (n = 91). At stimulus onset, the distribution of spike numbers evoked by catch trials versus trials with highest amplitude difference differed clearly in both single- and multi-unit data. However, at the end of the stimulus or taking the whole stimulus period into account, the difference in response to S- and the strongest S+ was mainly visible in multi-unit recordings (Figure 6B). The information about the stimulus in the steady state as revealed by the multi-unit data are likely the neuronal correlate of the minor psychometric performance when only intensity and frequency cues are present (Figures 3C,D and 4C).

[The detailed effect sizes of spike count distributions obtained comparing 0 (catch) and 7.2° difference amplitude (the strongest S+) and using different durations of integration windows are the following (effect size is expressed as AUROC, i.e., values of 0 and 1 indicate completely separated distributions and a value of 0.5 indicates identical distributions; values in-between describe distributions overlapping to different degrees). Below, the first number

depicts the effect size obtained with single-unit trains (n = 74) and the second the one obtained with multi-unit trains (n = 91) from animals working on Experiments 1a and b: stimulus onset: window 50 ms: 0.63, 0.81, window 100 ms: 0.63, 0.76, and window 200 ms: 0.68, 0.73. Stimulus end: window 50 ms: 0.56, 0.59; window 100 ms: 0.56, 0.62; window 200 ms: 0.60, 0.65. Entire stimulus period: 0.65, 0.73.].

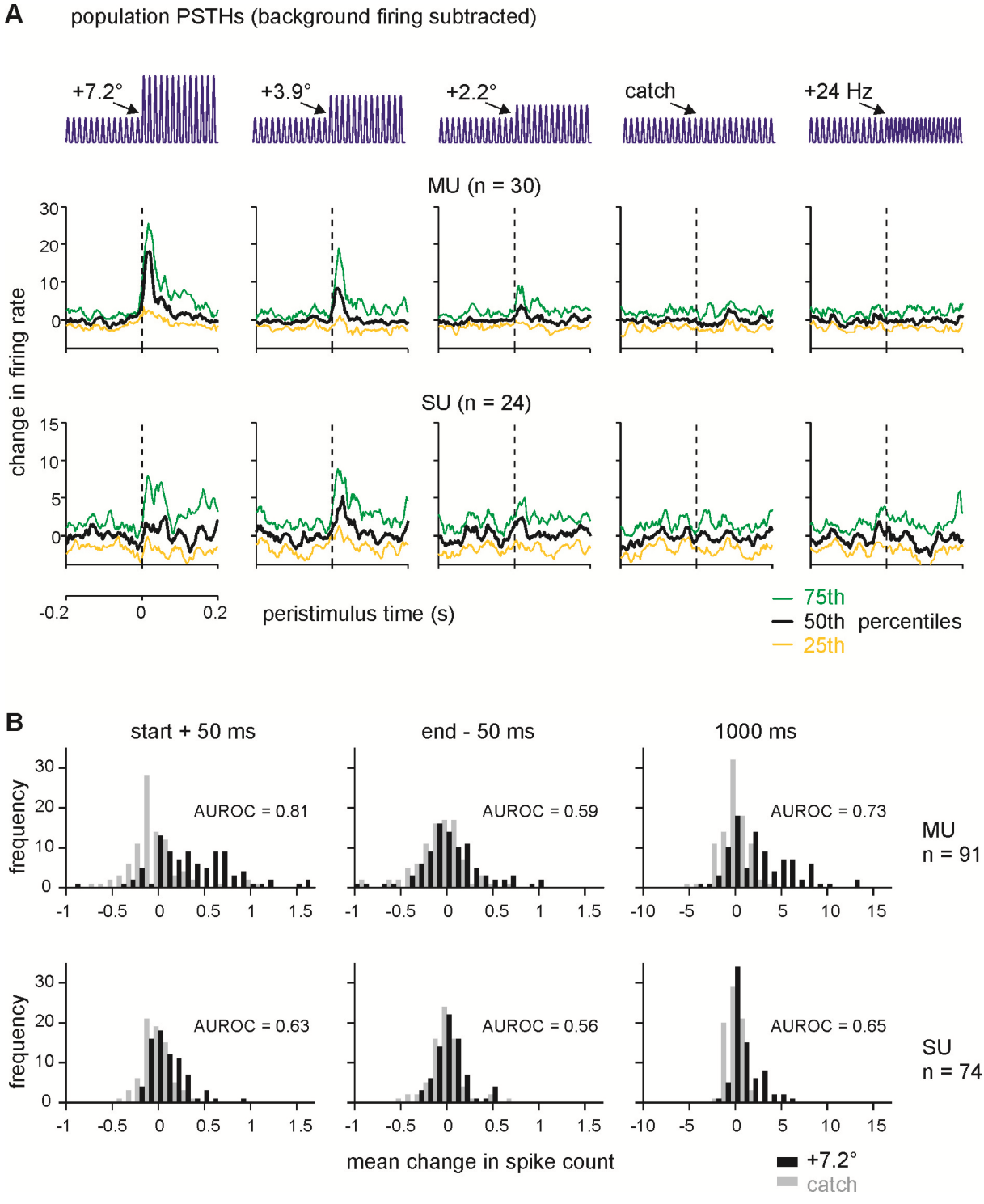
A
population PSTHs (background firing subtracted)
+7.2°
+3.9°
+2.2°
catch
+24 Hz
MU (n = 30)
SU (n = 24)
change in firing rate
peristimulus time (s)
75th
50th percentiles
25th
B
start + 50 ms
end - 50 ms
1000 ms
AUROC = 0.81
AUROC = 0.59
AUROC = 0.73
AUROC = 0.63
AUROC = 0.56
AUROC = 0.65
frequency
MU
n = 91
SU
n = 74
mean change in spike count
+7.2°
catch

*Figure 6. Population analyses of cortical responses to pulsatile stimuli. (*A*) Distributions of evoked activity across time (bin width 1 ms) for the whole population of units (multi-units,* n *= 30; single-units,* n *= 24) recorded in Experiment 1b. (Note that the ordinate scales responses as 'changes in firing rate' because the sustained firing rate to the S- background stimulus has been subtracted). Each subplot shows the unitary responses to a different S+ stimulus or catch trial (schematized on top). The curves indicate the median (black) and the 75th (top) and 25th (bottom) percentile (yellow and green). Note that the firing rate distributions labeled '+24 Hz' were the ones obtained with the extra stimuli of Experiment 1b, in which frequency was manipulated and waveform kept constant (cf. Fiure 3*D*). These responses, although obtained in Experiment 1b, in fact belong to the same category of stimuli as the ones used in Experiment 2a. (*B*) Distributions of neuronal activity evoked by the strongest amplitude change (7.2°, black bars) and catch trials (gray bars) as observed in Experiments 1a and b. The abscissa scales response as spike counts in three different intervals. Left: immediately after stimulus onset (0-50 ms peristimulus time). Center: before the stimulus offset (950-1000 ms peristimulus time). Right: the whole stimulus period (0-1000 ms peristimulus time). Multi- (MU,* n *= 91, top) and single-unit data (SU,* n *= 74, bottom) are shown.*

My next aim was to estimate the integration interval employed by the perceptual read-out using quantitative comparison of the neurometric with the psychometric data. The hypothesis that instantaneous kinematic cues are the main basis of perception would be strengthened by the finding of short optimal integration windows. To this end, the distributions of single-trial spike counts were converted to neurometric sensitivities, again by applying ROC analysis (see Materials and Methods; note that for the present purpose of calculating sensitivities, AUROC values are used to compare single-units' ability to discriminate a stimulus pair on the basis of single trials while, in the section before, AUROC was used as a measure of effect size for the comparison of mean responses measured across the sample of units). Neuronal sensitivities with which each S+ could be discriminated from S- were then compared with the respective psychometric sensitivities calculated from the rat's lick responses in the same sessions. Panel A of Figure 7 plots AUROC values for all single-units (gray) recorded in Experiment 1b (AUROC values of 0.5-1 scale chance to perfect discrimination if cells are excited, while values of 0.5-0 scale the same in the case of inhibitory responses). The psychometric curve shown in blue (identical for all subplots) is the average across three rats. Each subplot illustrates the neurometric performance based on spike counts taken from integration intervals starting at the stimulus onset but with different durations. The few responding neurons showed a tendency to increase sensitivity with increasing amplitudes, but did so in highly variable ways. Some of them showed low, others rather high amplitude thresholds to reach elevated sensitivity. However, even those who did respond stayed far below the performance of the rat. One reason for the poor neuronal sensitivity was their low spike number per trial, especially when using small encoding windows. In a 20-ms window, for example, the spike count was mostly zero and virtually did not exceed one or two spikes. In addition, neuronal sensitivity did not vary significantly across cortical depth. Units grouped into three bins indicating roughly superficial (400-800 µm), middle (800-1200 µm), and deep (1200-1700 µm) locations (as measured by screw turns at the electrode array) showed similar mean AUROC values for the discrimination of the strongest S+ stimulus from S- [mean ± SD; 0.57 ± 0.13 (n = 44), 0.61 ± 0.12 (n = 84), and 0.59 ± 0.10 (n = 37); t-test for independent samples, all three pair-wise comparisons $P > 0.05$]. In conclusion, responses of individual barrel cortex neurons contain low sensitivity for the task, and thus, provide a poor tool to estimate the integration interval. Individual neurons are unlikely to be at the basis of the animals' discrimination performance. To

explore whether the psychometric results can be better explained by population activity, and thus allow a better estimate of the optimal integration interval, I fitted a probabilistic model that computes the likelihood function of neurons within a pool under the assumption of independence (Figure 7B) as done previously (Jazayeri and Movshon, 2006; Stüttgen and Schwarz, 2008). The pool neurons were modeled based on the single-unit data obtained in Experiments 1a and b. Using a Monte Carlo procedure, I varied 1) the duration of the spike count window, 2) the number of most sensitive neurons picked to compose the pool, 3) the pool size, and 4) the animal's expectation, that is, the prior ratio. The first parameter, the spike count window, is the most important one for the present purpose, because it gives us an estimate of the optimal integration interval. Parameters 2 and 3 are important as they hint at spatial specifications of optimal readout mechanisms. With low optimal number of neurons selected and used for the pool, read out mechanisms that assess neurons in highly specific ways are better than unspecific ones. Lastly, the fourth parameter addresses the expectation of the animal. In the behavioral sessions, the animals experience favorable times (presence of S+ and availability of reward) and unfavorable times (absence of S+, i.e., presence of S-). The trained animal, thus, forms an expectation of the presence S+ through learning and uses it (e.g., to adjust lick rates) even before perceiving the sensory stimuli. Under the Bayesian framework, incoming actual sensory data are integrated with this prior belief to take a decision (equations 4 and 5). A low value of this parameter would indicate that the animals count trial numbers of S- and S+ to calculate their prior belief. A high value speaks in favor of the alternative strategy, to measure presentation times of S+ and S-. Refer to Materials and Methods for more details and the justification of each parameter's range in which values were varied to fit the model.

The single-units in the dataset were ranked according to their sensitivity to discriminate the strongest stimulus changes. In each resampling step, spike responses of randomly chosen units were drawn based on the measured firing probabilities, and the log-likelihood function was computed for each neuron. The log-likelihood function of the whole population was then calculated by summing the contributions of individual neurons. In the last step of each simulation, a decision rule was applied that compared likelihoods of S+ and S- stimuli, taking into account varying prior probabilities of the absence or presence of a stimulus (see Materials and Methods for more details). The goodness of fit of the simulated pool-

neurometric curves with the psychometric ones was estimated by calculating their Euclidean distance. Figure 7C shows the best fit results for Experiments 1a and b, respectively. The simulated pool response curve with the best fit is shown as dashed line, whereas psychometric data are shown as solid line. Both, neurometric and psychometric data are shown as a function of amplitude difference for the six core stimuli, although the best fit was calculated for the whole stimulus set including additional stimuli that modulated intensity or frequency (cf. Figure 3C,D). There was a consistent underestimation of the catch trial performance of the neuronal pools, in line with the notion that the neurons were purely sensory driven and did not reflect the (presumptive top-down) neuronal correlate of the animal's impulsivity. Across experimental conditions 1a and b, I found that the model robustly fitted the free parameters at optimal pool size of 10 neurons, the usage of the three most sensitive neurons (located at a depth of 930-1325 µm), and a prior ratio of 7.6. A pool consisting of more than 10 neurons led to an increase in neuronal sensitivity, which was exceeding the performance of the animal, leading to a larger Euclidean distance and a worse fit of the model. The low number of pool neurons (and the usage of a small number of sensitive neurons) speaks in favor of the notion that very few neurons can carry enough information to explain the performance of the subject as noted before (Stüttgen and Schwarz, 2008, 2010). The optimal prior ratio of 7.6 was closer to the value of 10.5 expected if the animals measure absolute durations of S+ versus S- presentations than the one expected from using a ratio of trial numbers for this calculation (value 0.13 or 0.17 for Experiments 1a and b, respectively). This finding is reasonable, because the trial-based structure of the DOC task is not easily assessable for the subject: S- trials have low probability to be noted consciously (they lead to a longer period of perceived background stimulation), and, therefore, are unlikely to contribute to a generation of a prior belief based on trial numbers. The most important finding of the modeling exercise was that the optimal spike count window was of short duration and ranged between 50 and 200 ms (indicated by small Euclidean distances in Figure 7D, note that a higher Euclidean distance indicates a mismatch between neurometric and psychometric curves irrespective of which of the two is better or worse in absolute terms). The finding of short integration windows might have been expected from the strong response adaptation of firing rates, reported above. It is interesting to note, however, that the best fit interval is somewhat longer than the peaks of spiking activity in the PSTHs, likely reflecting the information contained in tonic increment of

the firing rate as observed in some units (cf. Figure 6B). In summary, these results suggest that the decision of the animals requires a small population of cells and is possible using fast and transient responses. Such a coding scheme seems adequate to process instantaneous kinematic cues which, as shown by the psychophysical analysis, are the essential parameter used for the performance on the DOC task.

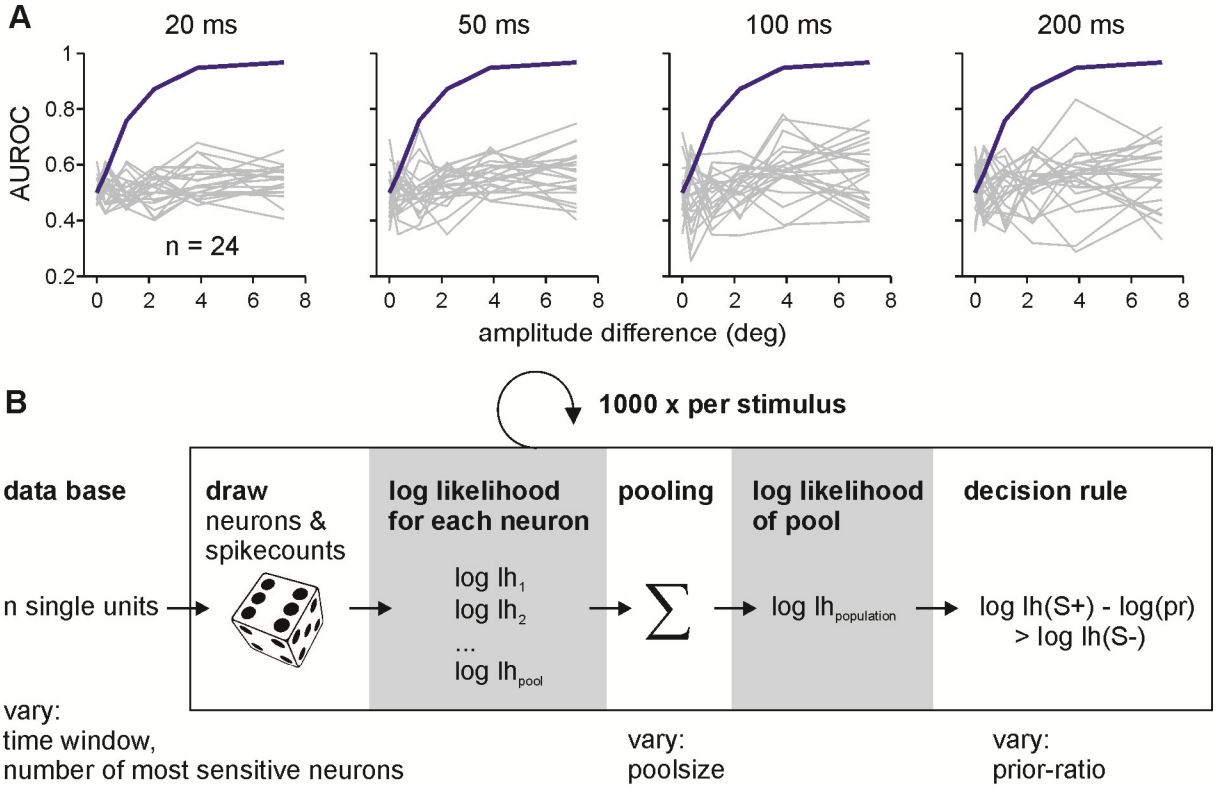
A
20 ms
50 ms
100 ms
200 ms
AUROC
n = 24
amplitude difference (deg)
B
1000 x per stimulus
data base
draw
neurons &
spikecounts
log likelihood
for each neuron
pooling
log likelihood
of pool
decision rule
n single units
log lh1
log lh2
...
log lhpool
log lhpopulation
log lh(S+) - log(pr)
> log lh(S-)
vary:
time window,
number of most sensitive neurons
vary:
poolsize
vary:
prior-ratio
C
Experiment 1a
Experiment 1b
response probability
psychometrics
best fit neurometric model
amplitude difference (deg)
D
# sensitive neurons = 3
poolsize = 10
prior ratio = 7.6
Eucl. dist.
time window (ms)

Figure 7. Quantitative comparison of neurometric and psychometric curves to estimate the optimal integration interval used to generate a percept. (A) Neurometric sensitivity of single neurons. The graphs show neuronal sensitivities based on spike count distributions observed within integration intervals of different durations starting at stimulus onset (top). The neurometric (gray lines) and psychometric (blue line) sensitivities are plotted as the function of changes in stimulus amplitude (pairwise comparisons to catch trials) and are expressed as area under the ROC curve (AUROC). The psychometric sensitivity is calculated as the mean across three animals subjected to Experiment 1b. Single neuron's activity cannot explain the animals' performance as none reached the psychometric sensitivity, irrespective of the integration interval used. (B) Performance of neuronal pools. A Monte Carlo procedure was used to fit the neurometric performance of a population of neurons to the psychometric performance. Random picks from the measured spike count distributions of pool neurons, were converted into log likelihood functions and summed up to yield the pooled log likelihood (lh) function and the pool's decision (equation 5). Repeating the procedure 1000 times yielded the pool's response probability. Four variables were varied to find the best fit of the pool response to the psychometric performance: 1) the duration of the integration interval, 2) the number of neurons in the pool, 3) the number of sensitive neurons chosen for read-out, and 4) the prior belief of the animal. (C) Optimal model performance was assessed by calculating the Euclidean distance between the outcome of each combination of model variables and the psychometric performance in Experiments 1a and b. The best fits of pool neurometric sensitivity (broken lines) are plotted together with the average psychometric curve (solid colored lines) of the three rats. (D) Model performance as a function of the integration interval. The three other variables (listed on top) were fixed to their best fits, which were found consistently in Experiments 1a and b. Smallest Euclidean distances (Eucl. dist.) were found for intervals between 50 and 200 ms. The best fits are indicated by arrows. Note the log scale of the abscissae.

3.3. Psychometrics with 'slip-like' events and background noise

The second psychophysical dataset (experiment 3-5) was sampled from 7 rats each subjected to a DOC paradigm (Figure 2B). Rat 7 and 8 were first trained on the detection of broadband noise against no movement (experiment 3) and then were subjected to a task in which they were required to detect multiple (6 to 20 per second) pulsatile kinematic events as described in the methods section. As the kinematic profile of these events was chosen to resemble slip events occurring with active palpation of textures (Wolfe et al., 2008), I tag them 'slip-like' events. All other animals (rats 9-13) were immediately trained on the latter task. At the end of training the number of events was reduced to one (single ramp-like events or single pulse-like events, cf. table 2) in all subjects. In a subset of animals (rats 8-11) the task was then refined for systematic psychometric assessment of pulse amplitude (A_f) and number (N_f) as described in experiment 5. All variations of the DOC task presented here were readily learned by the rats that were trained on them. For purposes of logic of presentation I will describe experiment 4 before experiment 5 although they were actually performed in reverse temporal order.

Experiment 3 aimed at identifying a background noise level that is perceivable but does not saturate the sensory system. The two animals learned to detect the presence of a noisy whisker deflection of 1 s duration (S+) which varied in amplitude A_n (Figure 8A). When the animal detected the presence of noise and reported it by a lick during the 1 s presentation time (Hit response), it obtained a water reward. Catch trials contained no whisker movement (S-); lick responses during a 1 s long period (false alarm, FA) were not rewarded. The psychometric curves assessed this way indicated that a noise level with 2*SD = 1° would be readily perceptible. Its location on the supra-threshold, sloped portion of the psychometric curve however assures that it engages the tactile system without driving it into saturation (Figure 8B).

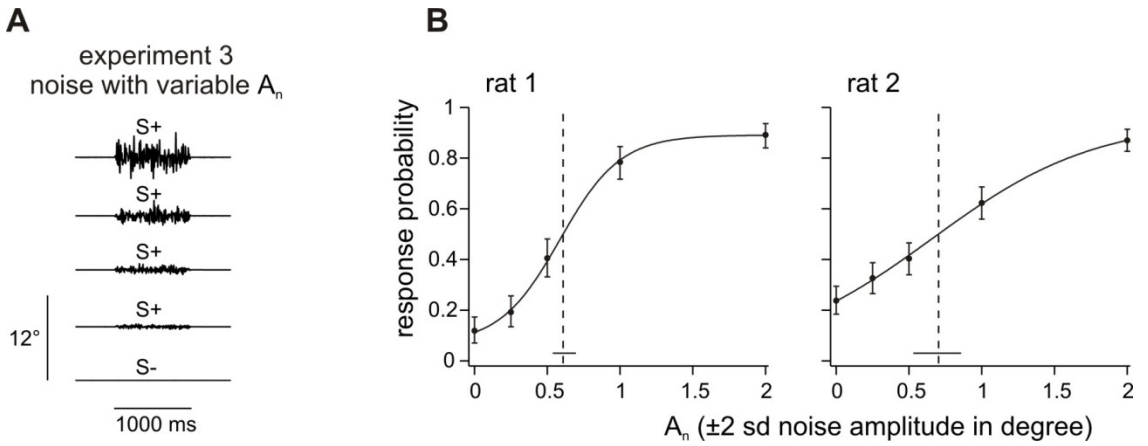

Figure 8. Broadband noise detection. (A) 1s of broadband noise with different amplitudes (A_n) was presented pseudo randomly in a trial based fashion in experiment 3. The task of the animal was to detect any whisker deflection. (B) Response probabilities of 2 rats are depicted as a function of noise amplitude (A_n). Data points represent means (n = 154-230 trials per stimulus, 5-6 sessions) and smooth lines are logistic fits estimated from a maximum likelihood estimator. Vertical error bars represent 95% confidence intervals. Horizontal bars at the bottom represent 95% confidence intervals of the thresholds (dashed line).

Experiment 4 was designed to test the animals' ability to discriminate single 'slip-like' events from a noisy background. Experiments 4a and b (Figure 9A and B) tested whether the exact waveform (pulse vs. ramp) of the 'slip-like' event matter for perception. These experiments kept the background noise level A_n constant at a well perceptible level of 2*SD = 1° as assessed in experiment 3. Experiment 4c (Figure 9C and D) was designed to investigate whether and how detection of 'slip-like' events are dependent on the intensity of the background noise. In this experiment ramp-like events were embedded into noise of different standard deviations in separate sessions. For all sub-experiments within experiment 4, a single 'slip-like' event (S+) was embedded into continuous background-noise every 4 to 10 s (Figure 2F and 9AC). When the animal detected a 'slip-like' event and reported it by a lick during a 1 s time window following the occurrence of the event (Hit), it obtained a water reward. Catch trials contained a continuation of the background noise (S-) without any embedded event and lick responses within a 1 s period (FA) were not rewarded. All sub-experiments of experiment 4 together, clearly established that rats can readily detect single 'slip-like' events embedded in noise, as psychometric curves were typically characterized by Hit rates above 0.8 and FA rates of ~0.2 (Figure 9BD). Experiment 4a and 4b

tested detection performance with pulses vs. ramps (Figure 9AB). The waveforms of the uprising phases of pulses and ramps were congruent while they differed in the downswing. Pulses were mirror-symmetric with respect to the vertical line through their peaks while ramps returned to zero on a very slow trajectory which does not lead to primary afferent activity and cannot be perceived by rats (Stüttgen, 2006) (see waveforms in Figure 2F). One animal (rat 7) received both, pulses and ramps of identical amplitudes (A_f) and maximal velocity, in alternating sessions (Figure 9B left). The other rats were trained either on ramps or on pulses (Figure 9B right; n = 3 for each group, cf. table 2). The psychometric curves obtained with pulses and ramps were almost identical, suggesting that reaching a critical speed once (i.e. with ramps) was sufficient to reach the detection performance seen with pulses in which the maximum speed occurred twice. In order to test how detection of slip events relates to the relative noise amplitude, I conducted experiment 4c using varying noise amplitudes (A_n) and respectively scaled the amplitudes of the 'slip-like' features (A_f) (Figure 9C). I found that the signal-to-noise ratio was no unique determinant of perception. Higher absolute feature amplitudes (velocities) were detected far better than lower ones even when relative noise amplitudes were adjusted to be constant. On the other hand, perception was not entirely independent of absolute noise amplitudes (as expected from the simple fact that event amplitudes tend to vanish into the noise with increasing noise amplitudes): the same event amplitudes (velocities) were detected somewhat better with lower as compared with higher noise amplitude. Figure 9D suggests that it is the difference of event and noise amplitude, which determines perception. Plotting perceptual performance across this difference, results in very similar psychometric curves and statistically inseparable thresholds. In summary, experiment 4 provides evidence for the notion that, for detection of an event, the animals use its maximum amplitude/velocity after subtraction of the amplitude of ambient noise.

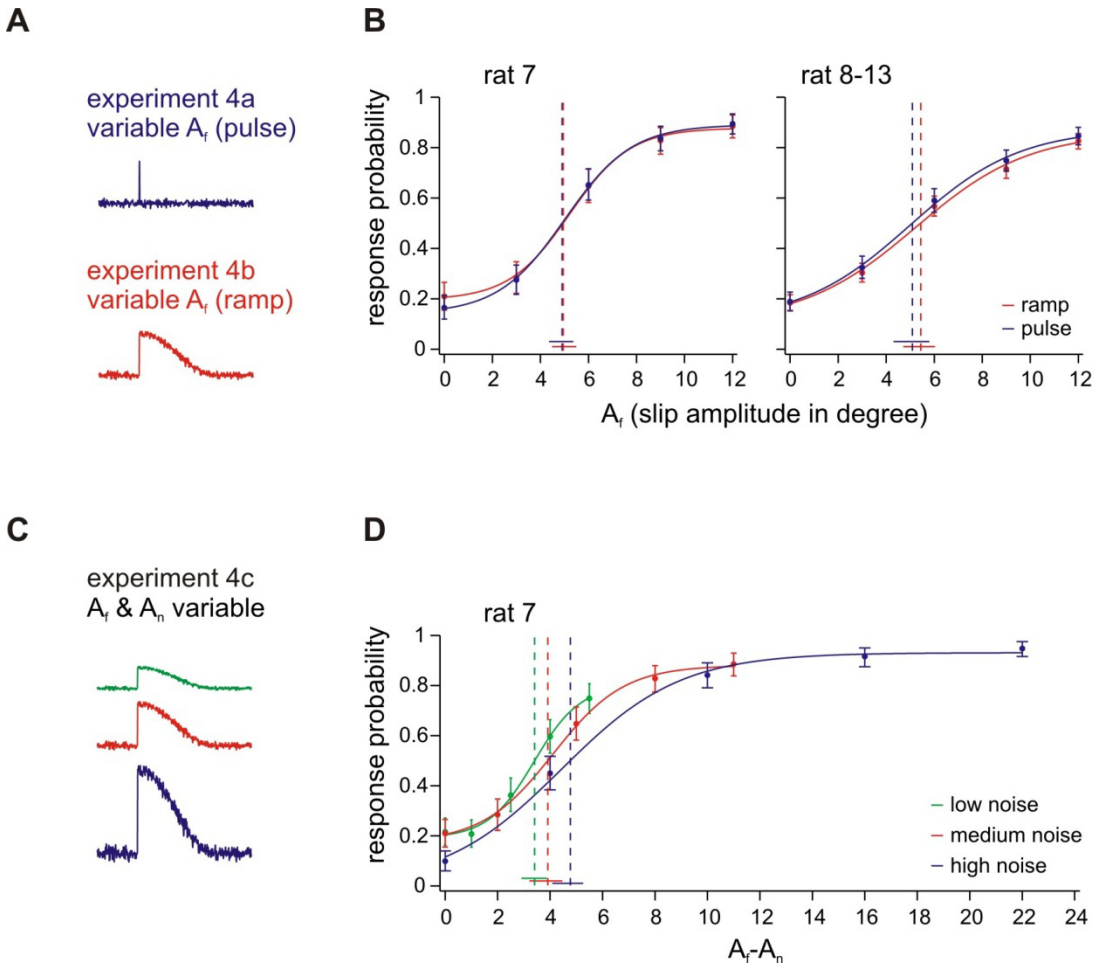

Figure 9. Pulse vs. ramp detection. (A) 'Slip-like' features of different amplitudes (A_f) and shape were embedded into broadband noise. The events consisted either of pulses (single-period sine wave; 100 Hz; duration 10 ms, experiment 4a) or ramps (half-period sine wave; duration 5 ms with 995 ms decay, experiment 4b). B. Left: Psychometric curves from one animal detecting pulse and ramp stimuli in alternating sessions (n = 196-226 trials per stimulus, 8-9 sessions). Right: Psychometric curves from three animals with pulse stimuli vs. three animals with ramp stimuli. Response probabilities are averaged across subjects and sessions (n = 427-593 trials per stimulus, 17-22 sessions). C. In experiment 4c the background noise level (A_n) was varied between sessions and amplitudes of 'slip-like' features (A_f) were scaled accordingly. D. Psychometric performance of one animal extracting 'slip-like' features from background noise in three different amplitude ranges (n = 196-203 trials per stimulus, 8-9 sessions). Detection probability is plotted as a function of amplitude difference between feature and noise (A_f-A_n). Curve fit and error bar conventions as in Figure 8.

Finally in experiment 5, I tested the perceptual capabilities of 4 animals (rat 8-11) to extract 'slip-like' features of different amplitudes (A_f) and numbers (N_f) from the background noise (Figure 10A). The animals were allowed to immediately report the first event after it had occurred. As noted before, all animals received initial training using multiple pulses before being subjected to experiment 5 to provide them with the possibility to learn to use temporal integration, if they could. Single event testing always came last in the training sequence. If the animals integrated across 'slip-like' events, one would expect higher response rates for trials with a higher N_f and prolonged reaction times. However, the presence of multiple 'slip-like' events only slightly improved Hit rates (red and green curves in Figure 10B) above the ones observed with single events (blue curves) with a non-significant increase of perceptual thresholds (as indicated by overlapping 95% confidence intervals). Evaluation of reaction times (interval between a 'slip-like' event and the rewarded lick) further revealed that a majority of successful licks were hardly affected by N_f. Figure 10C shows typical lick time distributions from one animal relative to the n^{th} event of a trial (from top to bottom: sixth, third, first 'slip-like' event) with intermediate amplitude (A_f = 6°). Reaction times to the first event were found to be in the typical range as measured in simple detection tasks using single pulses (Stüttgen and Schwarz, 2010) and also matched the ones obtained in this study with trials exclusively presenting single events per trial (experiment 4). If licks are plotted in relation to the second and third event, the distributions become more spread in time and move towards zero. With higher numbers (N_f > 3) the relative lick times become negative indicating that these 'slip-like' events were not causally related to the indicator response. Figure 10D shows median reaction times as well as interquartile ranges for all possible stimuli and for all animals used in this experiment (separated by colors). As seen in the example before, the first 'slip-like' event triggers a majority of lick responses at delay overlapping with the responses to single pulses from experiment 4; whereas the following events cannot account for most of the lick responses, since the relative lick times are too small or even negative, a result that is consistent across feature amplitudes and subjects. I conclude that although the animals have been trained on multiple 'slip-like' events, they do not integrate the vibrotactile signal to optimize perception.

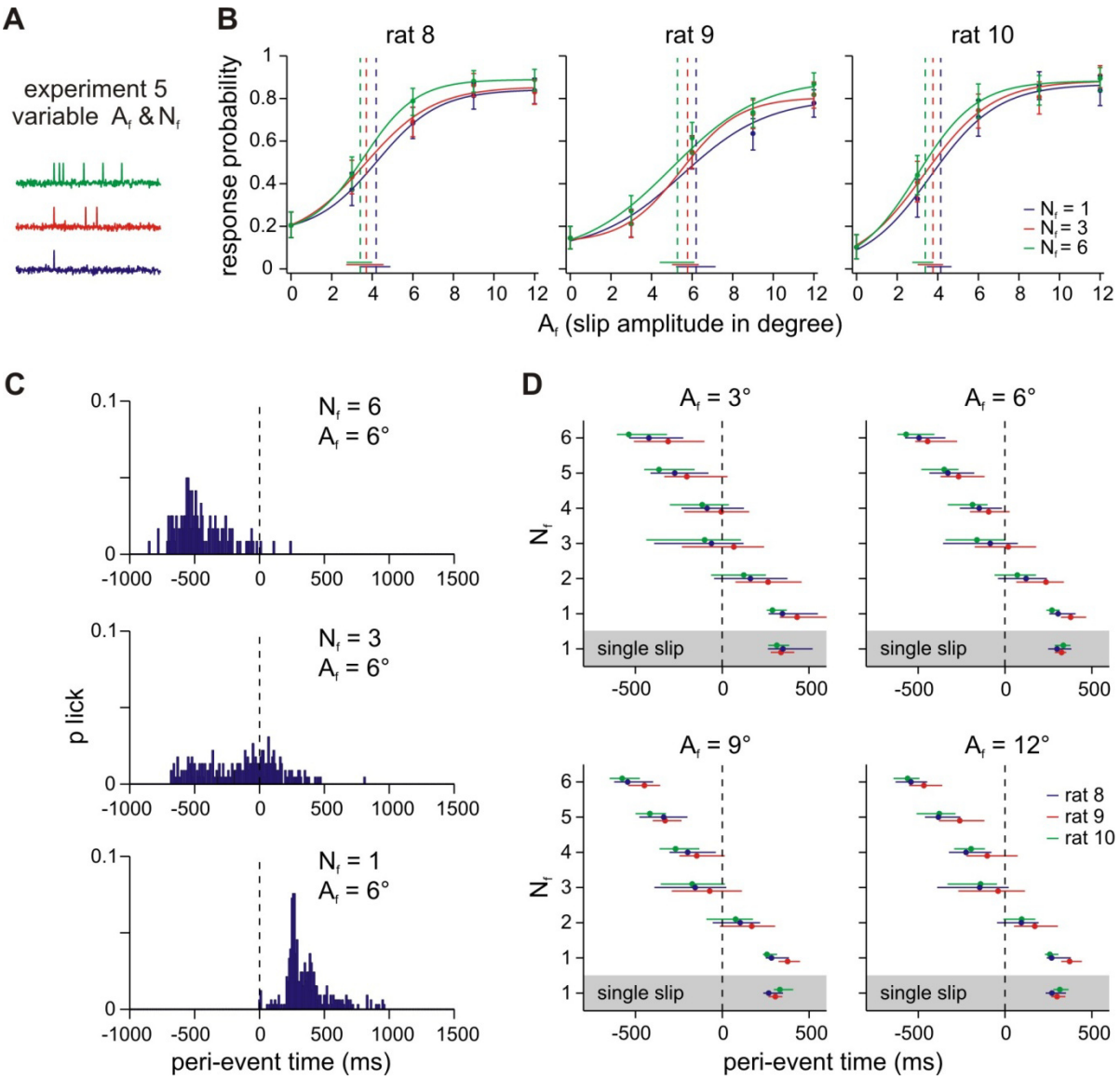

Figure 10. Effect of slip number on perception. (A) Example trials from experiment 5 with different numbers of embedded 'slip-like' features (N_f). They were presented within a maximal window of 1 s which also represented the time window for response and potential reward. The time window was always initiated by the first event and the following events were distributed randomly with a minimal distance of 50 ms peak to peak. (B) Psychometric curves of three animals performing the DOC task with 'slip-like' features varying in number (N_f) and amplitudes (A_f). Each data point represents the mean response probability as a function of A_f (n = 105-164 trials per stimulus, 10-13 sessions). Curve fit and error bar conventions as in Figures 8 and 9. (C) Histograms of one animal's lick times relative to the n^{th} slip of a trial (from top to bottom: N_f = 6, 3, 1) with intermediate amplitude (A_f = 6°). (D) Median reaction times and interquartile ranges for all animals and all stimuli (Subplots separate different A_f, subjects are color coded). Median reaction times to single events from experiment 4 are also shown for comparison (inside grey box).

4. Discussion

4.1. Support for neuronal coding of instantaneous kinematic cues

The present psychophysical and electrophysiological measurements demonstrate, for the first time, that neuronal representations of kinematic events, extracted from instantaneous kinematic variables of whisker trajectories, play a decisive role for the subject's performance in a tactile discrimination task. Changes in pulsatile stimuli in the DOC format were detected well by animals as well as barrel cortex neurons, given the switch was characterized by a change in instantaneous kinematic cues. In contrast, if the stimulus switch was based exclusively on the classical parameters frequency and intensity, the performance of animals and neurons was minor. How can these results, clearly favoring instantaneous extraction of kinematic events, be brought into register with previous evidence presented for each of the three candidate parameters? The original evidence for the 'frequency' and 'intensity' hypothesis comes from the primate literature on perception of 'flutter'. Classic experiments have shown that the perception of 'intensity' and 'pitch', reported by human observers, cannot unequivocally be attributed to single stimulus parameters like amplitude and frequency of a sine wave (LaMotte and Mountcastle, 1975). My perceptual measurements in the whisker system using seamless switches of pulsatile whisker vibrations were aimed to disentangle instantaneous and time integrated parameters (i.e., instantaneous kinematic cues and mean speed) which had been conflated by the amplitude changes of sine wave stimuli in the older literature. The present data clearly show a high level of psychophysical performance whenever instantaneous kinematic cues were present and a diminished one whenever these cues were absent. Thus, I could not find strong evidence for dominant perceptual qualities of pitch and intensity as conjectured in the primate hand system. In my view, this does not exclude the possibility that both systems share mechanistic principles of tactile processing. First, the classic studies, unable to separate the contribution of instantaneous versus time integrated parameters, may have ignored the contribution of instantaneous cues. Second, the similarity of instantaneous coding in primate hand and rodent whisker systems found more recently (Mackevicius et al., 2012) suggests a read-out of such information for perception. Finally, the insight that vibrissae and skin represent bioelastic elements, both capable of adding instantaneous kinematic cues about the probed

texture to the vibrotactile signal (Scheibert et al., 2009; Jadhav and Feldman, 2010), support my expectation that future work may well reveal a significant role of instantaneous kinematic cues for primate vibrotactile perception as well.

The intensity hypothesis has received great biomechanical evidence also in the whisker system: the power of the vibrotactile signal (another possible measure of intensity) has been shown to carry a large amount of information about the roughness of the contacted texture (Hipp et al., 2006). Psychophysical evidence using a trial based Go/No Go paradigm showed that rats used intensity cues while being unable to use frequency and instantaneous kinematic cues offered to them (Gerdjikov et al., 2010). The present data using the DOC paradigm are in accordance with a role of intensity cues. However, the prominence of the instantaneous kinematic cues for discrimination performance shown here raises the question as to why the importance of this parameter was ignored by the previous study. One possibility is that the cognitive process model (Stüttgen et al., 2011) of the previous task contains a step in which stimulus information must be stored in long-term memory. In each trial, the animal observes only one stimulus which it compares to the S+ stored in long-term memory during learning of the task (the memory period in the Gerdjikov study was the time difference between the current trial and the last S+ trial successfully discriminated, i.e., minimally one interstimulus trial of 15–25 s). Considering the need to limit the size of content stored in memory due to capacity limits, it is conceivable that only a strongly compressed version of the vibrotactile signal is being preserved. This is exactly what was found: intensity, the average of the speed trajectory rather than the full trajectory, is what the animals used for discrimination (Gerdjikov et al., 2010). A second line of evidence in favor of intensity is based on recordings in urethane-anesthetized rats (Arabzadeh et al., 2003) which showed that neuronal spike counts in barrel cortex can neither be aligned with frequency nor with the amplitude of sinusoidal stimulation alone. In that study, long intervals of spiking were analyzed ignoring transient responses. In contrast, the present study shows that information about the awake animal's choice is largely contained within the first 200 ms after stimulus change, that is, in the transient response. I therefore conclude that the analysis of a long stimulus period — at least under the present experimental conditions — does not lead to an adequate description of neuronal activity used for perception. Another neurophysiological study using repetitive pulsatile whisker stimulation

observed that neuronal responses to stimuli with varying ('noisy') pulse amplitudes are larger than those to stimuli containing constant pulse amplitudes (Lak et al., 2010). However, in this study responses to individual pulses showed also a clear tuning toward higher pulse amplitudes (or velocities) which in principle is as well compatible with instantaneous evaluation of pulse amplitudes to be able to discriminate noisy from non-noisy stimuli. A more recent psychophysical study in freely running rats simultaneously presented sinusoidal whisker deflections on each side of the face, whose frequency (f) and amplitude (A) could be either low (f, A) or of double value (2f, 2A)(Adibi et al., 2012). The main point of that study was that animals failed to discriminate stimuli whenever the two variables were varied in the opposite direction (i.e., f/2A vs. 2f/A), which led Adibi and coworkers to conclude that discrimination cannot be based on f or A but rather on their product f*A which is proportional to the intensity (mean speed) in sinusoidal stimuli. Importantly, my present results show, that the conclusion of Adibi et al. is not the only valid interpretation of their result. The distributions of instantaneous velocities contained in the four stimuli (f/A, 2f/A, f/2A, 2f/2A) are identical (because all are sinusoids), but are differently scaled: f/A is characterized by the slowest maximum velocities, 2f/A and f/2A yield intermediate (but identical) maximal velocities, and 2f/2A gives the highest maximal velocities. Therefore, if the animals detected instantaneous velocities, instead of f*A, the result of Adibi et al. would have been the same. However, the question remains why the animals did not use amplitude differences (A vs. 2A) as discriminant cues. One possible answer is that the quite small amplitudes applied in that study (13 vs. 26 µm at the whisker tips, which gave rise to a low discrimination performance of max. ∼75%), activated exclusively rapidly adapting primary afferents, which have been reported to scale their response with velocity and are insensitive to amplitude (Stüttgen et al., 2006). From these considerations, I conclude that the results of Adibi et al. are well compatible with the notion that the animals use instantaneous kinematic cues for vibrotactile discrimination.

4.2. Support for the slip hypothesis

To pursue the slip hypothesis, I tested how subjects actually perform the DOC task when confronted with very short and single trial 'slip-like' sequences as sampled from different textures. The results obtained with these naturalistic stimuli provide behavioral evidence that rats are readily able to extract 'slip-like' events from background noise. I show that rats use instantaneous kinematic aspects of the embedded features rather than evaluating their waveforms or number. Again, temporal integration across the noisy signal plays a minor role for detection. It could be argued that the stimuli presented here are not ideal to prompt detection using integration as 'slip-like' events are presented at relatively low frequency. A simple modeling exercise shows that this objection is unfounded. I systematically investigated the ability of a series of models to detect 'slip-like' events, in which the temporal integration time was systematically varied. This was done by varying the duration of flat kernels (boxcar filters), which were used to filter the signal followed by application of a variable threshold to classify trials into hits ('slip-like' events present and detected) and misses ('slip-like' events present but not detected). The performance of such models is shown in figure 11A (full lines) together with the mean perceptual performance of the rats 8-10 (broken lines). The first observation is that 'slip-like' stimuli could be readily detected with small as well as with long integration windows. However, the models using small integration windows, i.e. the ones tuned to instantaneous signatures, fit the behavioral data best, as they reproduced the similarity of psychometric curves across the number of presented 'slip-like' events (different colors). The best fits for each window size were found by choosing the threshold that would minimize the largest deviation from the detection curves obtained from the rats. As shown in figure 11B, this minimum is quite different when using different integration windows. It is much smaller for short windows as compared to long ones. In conclusion, the modeling results firstly show that a strategy of temporal integration might not be effective to detect the stimuli used in this study, and secondly, lend further support to the hypothesis that rats in fact use instantaneous coding to detect rapid slip events in a noisy environment.

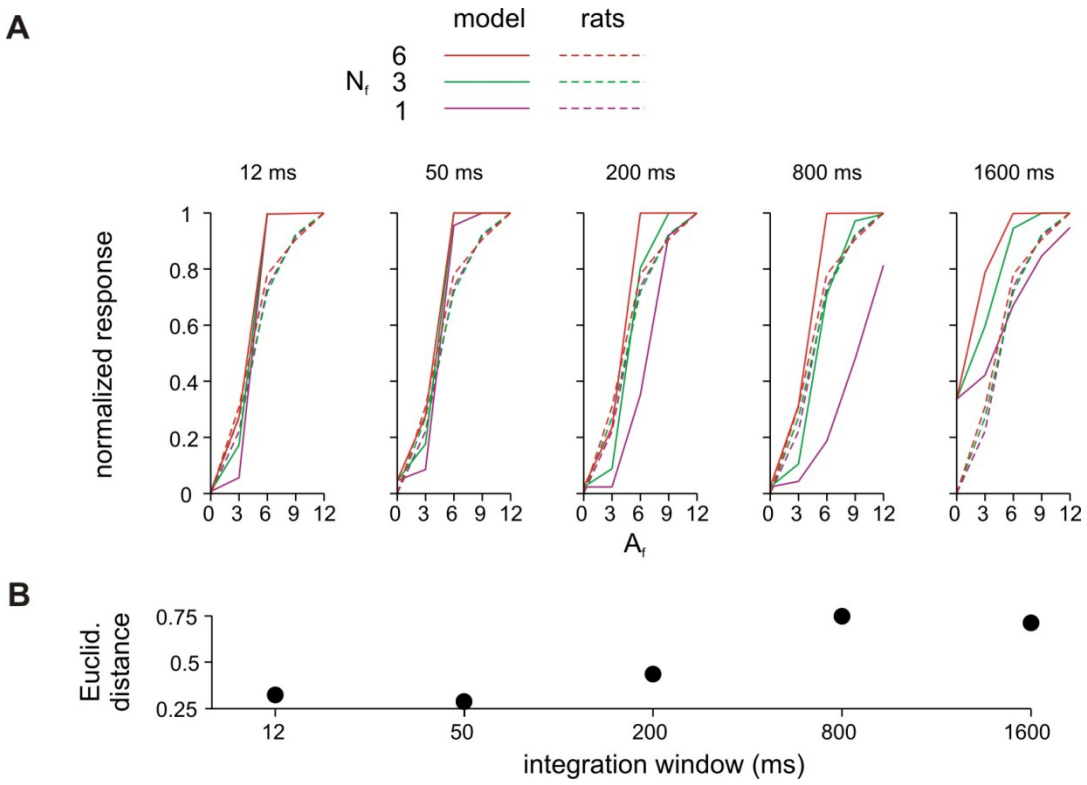

Figure 11. Integration model to detect 'slip-like' events. (A) Signal Integration with different temporal filters (boxcar filters) was used to classify trials into hits ('slip-like' events present and detected) and misses ('slip-like' events present but not detected). The model performance (full lines) is shown for five integration windows together with the actual mean perceptual performance of the rats (broken lines). Different numbers of 'slip-like' events (N_f) are separated by colors. (B) Comparison of detection thresholds between model and actual performance of the rats. The best fit (minimal Euclidean Distance) was obtained with a short integration window (50 ms).

In the present study I show that instantaneous encoding of kinematic signatures is used also in the presence of noise. This is important as neuronal adaptation to noise decisively changes stimulus responses. In whisker-related primary afferents, spike history clearly determines encoding properties of neurons (Chagas et al., 2013). Generally, several lines of evidence suggested that ongoing activity tends to reduce neuronal response to a given stimulus. Enhanced background firing during sensorimotor interaction (i.e. whisker movement) (Fanselow and Nicolelis, 1999; Hentschke et al., 2006) as well as pre-adaptation has been shown to lower tactile responses (Wang et al., 2010; Ollerenshaw et al., 2014). There is reason to believe that interactions can be even more diverse than simple suppression, as shown by complex interactions of stimulation of principal and surround

whiskers (Moore et al., 1999; Wilent and Contreras, 2005; Estebanez et al., 2012). However, adaptation does not simply work to adjust detection to the signal-to-noise ratio of the vibrotactile signal. It has been suggested to adjust the sensory system to better discrimination, but not detection of whisker deflections (Wang et al., 2010; Ollerenshaw et al., 2014). The present results suggest that the detection of 'slip-like' events is based on the difference of signal and noise rather than its ratio. A systematic appraisal of neuronal responses adapted to noise in an extensive range and its consequences for coding of kinematic events along the entire ascending tactile system is needed to tackle this question in the future.

In summary, my findings best fit the notion that rat whisker related tactile perception is based on instantaneous kinematic cues. Intensity cues (average speed) are less powerful and may be the parameter of choice if context demands (Gerdjikov et al., 2010). These results match the previous finding that for detection of repetitive whisker deflections, temporal integration is a minor factor. Temporal integration of short bursts of whisker deflections is limited to small integration windows, and even falls short of what is expected from simple probability summation (i.e., the probability to detect one of a number of single pulses presented in isolation) (Stüttgen and Schwarz, 2010). Small integration windows are in line with single-unit recordings in anesthetized animals which suggest that barrel cortex responses are transient and are most sensitive to whisker velocity (Pinto et al., 2000), that spiking on the ascending tactile pathway is precise and carries information about detailed features of the trajectory (Jones et al., 2004; Arabzadeh et al., 2006; Petersen et al., 2008; Chagas et al., 2013), and that such precise spiking is particularly useful to represent whisker slips — high amplitude/velocity/acceleration due to whisker elasticity (Arabzadeh et al., 2005; Ritt et al., 2008; Jadhav et al., 2009). The present results support the slip hypothesis as a theory of perception, as I show that detailed kinematic properties of single 'slip-like' sequences as sampled from different textures significantly optimize performance, whereas temporal integration across the signal plays a minor role. The prior finding that rats use the barrel cortex response to very few initial pulses after a stimulus switch to perform the DOC task stands in line with an instantaneous encoding mechanism during texture contact.

5. References

Adibi, M., Diamond, M. E., and Arabzadeh, E. (2012). Behavioral study of whisker-mediated vibration sensation in rats. *Proc. Natl. Acad. Sci. U. S. A.* 109, 971–6.

Arabzadeh, E., Panzeri, S., and Diamond, M. E. (2006). Deciphering the spike train of a sensory neuron: counts and temporal patterns in the rat whisker pathway. *J. Neurosci.* 26, 9216–9226.

Arabzadeh, E., Petersen, R. S., and Diamond, M. E. (2003). Encoding of Whisker Vibration by Rat Barrel Cortex Neurons : Implications for Texture Discrimination. *J. Neurosci.* 23, 9146–9154.

Arabzadeh, E., Zorzin, E., and Diamond, M. E. (2005). Neuronal encoding of texture in the whisker sensory pathway. *PLoS Biol.* 3, e17.

Berg, R. W., and Kleinfeld, D. (2003). Rhythmic whisking by rat: retraction as well as protraction of the vibrissae is under active muscular control. *J. Neurophysiol.* 89, 104–17.

Brecht, M. (2007). Barrel cortex and whisker-mediated behaviors. *Curr. Opin. Neurobiol.* 17, 408–16.

Brecht, M., Preilowski, B., and Merzenich, M. M. (1997). Functional architecture of the mystacial vibrissae. *Beh. Brain. Res.* 84, 81–97.

Britten, K. H., Shadlen, M. N., Newsome, W. T., and Movshon, J. A. (1992). The analysis of visual motion: a comparison of neuronal and psychophysical performance. *J. Neurosci.* 12, 4745–4765.

Carvell, G. E., and Simons, D. J. (1990). Biometric analyses of vibrissal tactile discrimination in the rat. *J. Neurosci.* 10, 2638–48. Available at: http://www.ncbi.nlm.nih.gov/pubmed/2388081 [Accessed February 26, 2014].

Chagas, A. M., Theis, L., Sengupta, B., Stüttgen, M. C., Bethge, M., and Schwarz, C. (2013). Functional analysis of ultra high information rates conveyed by rat vibrissal primary afferents. *Front. Neural Circuits* 7, 190.

Dörfl, J. (1982). The musculature of the mystacial vibrissae of the white mouse. *J. Anat.* 135, 147–54. Available at: http://www.pubmedcentral.nih.gov/articlerender.fcgi?artid=1168137&tool=pmcentrez&rendertype=abstract [Accessed March 4, 2014].

Ebara, S., Kumamoto, K., Matsuura, T., Mazurkiewicz, J. E., and Rice, F. L. (2002). Similarities and differences in the innervation of mystacial vibrissal follicle-sinus complexes in the rat and cat: a confocal microscopic study. *J. Comp. Neurol.* 449, 103–19.

Estebanez, L., El Boustani, S., Destexhe, A., and Shulz, D. E. (2012). Correlated input reveals coexisting coding schemes in a sensory cortex. *Nat. Neurosci.* 15, 1691–9.

Fanselow, E. E., and Nicolelis, M. A. (1999). Behavioral modulation of tactile responses in the rat somatosensory system. *J. Neurosci.* 19, 7603–7616.

Feldmeyer, D., Brecht, M., Helmchen, F., Petersen, C. C. H., Poulet, J. F. A., Staiger, J. F., Luhmann, H. J., and Schwarz, C. (2013). Barrel cortex function. *Prog. Neurobiol.* 103, 3–27.

Gerdjikov, T. V, Bergner, C. G., Stüttgen, M. C., Waiblinger, C., and Schwarz, C. (2010). Discrimination of vibrotactile stimuli in the rat whisker system: behavior and neurometrics. *Neuron* 65, 530–40.

Gibson, J. M., and Welker, W. I. (1983). Quantitative studies of stimulus coding in first-order vibrissa afferents of rats. 2. Adaptation and coding of stimulus parameters. *Somatosens. Res.* 1, 95–117. Available at: http://www.ncbi.nlm.nih.gov/pubmed/6679920 [Accessed March 4, 2014].

Haiss, F., Butovas, S., and Schwarz, C. (2010). A miniaturized chronic microelectrode drive for awake behaving head restrained mice and rats. *J. Neurosci. Methods* 187, 67–72.

Hartmann, M. J. (2001). Active sensing capabilities of the rat whisker system. *Auton. Robots* 11, 249–254.

Von Heimendahl, M., Itskov, P. M., Arabzadeh, E., and Diamond, M. E. (2007). Neuronal activity in rat barrel cortex underlying texture discrimination. *PLoS Biol.* 5, e305.

Hentschke, H., Haiss, F., and Schwarz, C. (2006). Central signals rapidly switch tactile processing in rat barrel cortex during whisker movements. *Cereb. Cortex* 16, 1142–56.

Hermle, T., Schwarz, C., and Bogdan, M. (2004). Employing ICA and SOM for spike sorting of multielectrode recordings from CNS. *J. Physiol. Paris* 98, 349–356.

Hipp, J., Arabzadeh, E., Zorzin, E., Conradt, J., Kayser, C., Diamond, M. E., and König, P. (2006). Texture signals in whisker vibrations. *J. Neurophysiol.* 95, 1792–9.

Hires, S. A., Efros, A. L., and Svoboda, K. (2013). Whisker dynamics underlying tactile exploration. *J. Neurosci.* 33, 9576–91.

Hutson, K. A., and Masterton, R. B. (1986). The sensory contribution of a single vibrissa's cortical barrel. *J. Neurophysiol.* 56, 1196–223. Available at: http://www.ncbi.nlm.nih.gov/pubmed/3783236 [Accessed March 4, 2014].

Jacquin, M. F., Chiaia, N. L., Haring, J. H., and Rhoades, R. W. (1990). Intersubnuclear connections within the rat trigeminal brainstem complex. *Somatosens. Mot. Res.* 7, 399–420.

Jadhav, S. P., and Feldman, D. E. (2010). Texture coding in the whisker system. *Curr. Opin. Neurobiol.* 20, 313–318.

Jadhav, S. P., Wolfe, J., and Feldman, D. E. (2009). Sparse temporal coding of elementary tactile features during active whisker sensation. *Nat. Neurosci.* 12, 792–800.

Jazayeri, M., and Movshon, J. A. (2006). Optimal representation of sensory information by neural populations. *Nat. Neurosci.* 9, 690–696.

Jones, L. M., Lee, S., Trageser, J. C., Simons, D. J., and Keller, A. (2004). Precise temporal responses in whisker trigeminal neurons. *J. Neurophysiol.* 92, 665–668.

Lak, A., Arabzadeh, E., Harris, J. a, and Diamond, M. E. (2010). Correlated physiological and perceptual effects of noise in a tactile stimulus. *Proc. Natl. Acad. Sci. U. S. A.* 107, 7981-6.

LaMotte, R. H., and Mountcastle, V. B. (1975). Capacities of humans and monkeys to discriminate vibratory stimuli of different frequency and amplitude: a correlation between neural events and psychological measurements. *J. Neurophysiol.* 38, 539–59. Available at: http://jn.physiology.org/content/38/3/539.abstract [Accessed March 5, 2014].

Lo, F. S., Guido, W., and Erzurumlu, R. S. (1999). Electrophysiological properties and synaptic responses of cells in the trigeminal principal sensory nucleus of postnatal rats. *J. Neurophysiol.* 82, 2765–2775.

Mackevicius, E. L., Best, M. D., Saal, H. P., and Bensmaia, S. J. (2012). Millisecond Precision Spike Timing Shapes Tactile Perception. *J. Neurosci.* 32, 15309–15317.

Mehta, S. B., Whitmer, D., Figueroa, R., Williams, B. a, and Kleinfeld, D. (2007). Active spatial perception in the vibrissa scanning sensorimotor system. *PLoS Biol.* 5, e15.

Miyashita, T., and Feldman, D. E. (2013). Behavioral detection of passive whisker stimuli requires somatosensory cortex. *Cereb. Cortex* 23, 1655–62.

Möck, M., Butovas, S., and Schwarz, C. (2006). Functional unity of the ponto-cerebellum: evidence that intrapontine communication is mediated by a reciprocal loop with the cerebellar nuclei. *J. Neurophysiol.* 95, 3414–3425.

Moore, C. I., Nelson, S. B., and Sur, M. (1999). Dynamics of neuronal processing in rat somatosensory cortex. *Trends Neurosci.* 22, 513–20. Available at: http://www.ncbi.nlm.nih.gov/pubmed/10529819 [Accessed October 10, 2014].

O'Connor, D. H., Clack, N. G., Huber, D., Komiyama, T., Myers, E. W., and Svoboda, K. (2010). Vibrissa-based object localization in head-fixed mice. *J. Neurosci.* 30, 1947–1967.

Ollerenshaw, D. R., Zheng, H. J. V., Millard, D. C., Wang, Q., and Stanley, G. B. (2014). The Adaptive Trade-Off between Detection and Discrimination in Cortical Representations and Behavior. *Neuron* 81, 1152–1164.

Pammer, L., O'Connor, D. H., Hires, S. A., Clack, N. G., Huber, D., Myers, E. W., and Svoboda, K. (2013). The mechanical variables underlying object localization along the axis of the whisker. *J. Neurosci.* 33, 6726–41.

Penfield and Rasmussen 1950 The Cerebral Cortex of Man. A Clinical Study of Localization of Function. *New York, Macmillan Comp, 1950*.

Petersen, C. C. H. (2003). The barrel cortex--integrating molecular, cellular and systems physiology. *Pflugers Arch.* 447, 126–34.

Petersen, C. C. H. (2007). The functional organization of the barrel cortex. *Neuron* 56, 339–55.

Petersen, R. S., Brambilla, M., Bale, M. R., Alenda, A., Panzeri, S., Montemurro, M. a, and Maravall, M. (2008). Diverse and temporally precise kinetic feature selectivity in the VPm thalamic nucleus. *Neuron* 60, 890–903.

Pinto, D. J., Brumberg, J. C., and Simons, D. J. (2000). Circuit dynamics and coding strategies in rodent somatosensory cortex. *J. Neurophysiol.* 83, 1158–1166.

Ramon Y Cajal (1911). Histologie du système nerveux de l'homme & des vertébrés. *Vols. 1 2. A. Maloine. Paris. 1911.* Available at: https://archive.org/stream/histologiedusyst01ram#page/n13/mode/2up [Accessed October 21, 2014].

Rice, F. L., and Munger, B. L. (1986). A comparative light microscopic analysis of the sensory innervation of the mystacial pad. II. The common fur between the vibrissae. *J. Comp. Neurol.* 252, 186–205.

Ritt, J. T., Andermann, M. L., and Moore, C. I. (2008). Embodied information processing: vibrissa mechanics and texture features shape micromotions in actively sensing rats. *Neuron* 57, 599–613.

Scheibert, J., Leurent, S., Prevost, A., and Debrégeas, G. (2009). The role of fingerprints in the coding of tactile information probed with a biomimetic sensor. *Science* 323, 1503–1506.

Schwarz, C., Hentschke, H., Butovas, S., Haiss, F., Stüttgen, M. C., Gerdjikov, T. V, Bergner, C. G., and Waiblinger, C. (2010). The head-fixed behaving rat--procedures and pitfalls. *Somatosens. Mot. Res.* 27, 131–48.

Simons, D. J. (1985). Temporal and spatial integration in the rat SI vibrissa cortex. *J Neurophysiol* 54, 615–635. Available at: http://jn.physiology.org/content/54/3/615 [Accessed March 4, 2014].

Stanislaw, H., and Todorov, N. (1999). Calculation of signal detection theory measures. *Behav. Res. Methods. Instrum. Comput.* 31, 137–149.

Stüttgen, M. C., Rüter, J., and Schwarz, C. (2006). Two psychophysical channels of whisker deflection in rats align with two neuronal classes of primary afferents. *J. Neurosci.* 26, 7933–41.

Stüttgen, M. C., and Schwarz, C. (2010). Integration of vibrotactile signals for whisker-related perception in rats is governed by short time constants: comparison of neurometric and psychometric detection performance. *J. Neurosci.* 30, 2060–2069.

Stüttgen, M. C., and Schwarz, C. (2008). Psychophysical and neurometric detection performance under stimulus uncertainty. *Nat. Neurosci.* 11, 1091–9.

Stüttgen, M. C., Schwarz, C., and Jäkel, F. (2011). Mapping spikes to sensations. *Front. Neurosci.* 5, 125.

Vincent, S. B. (1912). *The functions of the vibrissae in the behavior of the white rat*. Behavior Monographs 1: 1-86. Available at: http://books.google.de/books/about/The_functions_of_the_vibrissae_in_the_be.html?id=6m1MAAAAMAAJ&pgis=1 [Accessed March 4, 2014].

Waiblinger, C., Brugger, D., and Schwarz, C. (2013). Vibrotactile Discrimination in the Rat Whisker System is Based on Neuronal Coding of Instantaneous Kinematic Cues. *Cereb. Cortex*.

Wang, Q., Webber, R. M., and Stanley, G. B. (2010). Thalamic synchrony and the adaptive gating of information flow to cortex. *Nat. Neurosci.* 13, 1534–1541.

Welker, C. (1971). Microelectrode delineation of fine grain somatotopic organization of (SmI) cerebral neocortex in albino rat. *Brain Res.* 26, 259–75. Available at: http://www.ncbi.nlm.nih.gov/pubmed/4100672 [Accessed March 4, 2014].

Welker, W. I. (1964). Analysis of sniffing of the albino rat. *Behav. Leiden*. Available at: http://psycnet.apa.org/index.cfm?fa=search.displayrecord&uid=1965-01067-001 [Accessed March 4, 2014].

Wilent, W. B., and Contreras, D. (2005). Dynamics of excitation and inhibition underlying stimulus selectivity in rat somatosensory cortex. *Nat. Neurosci.* 8, 1364–1370.

Wolfe, J., Hill, D. N., Pahlavan, S., Drew, P. J., Kleinfeld, D., and Feldman, D. E. (2008). Texture Coding in the Rat Whisker System: Slip-Stick Versus Differential Resonance. *PLoS Biol.* 6, e215.

Woolsey, T. A., and Van der Loos, H. (1970). The structural organization of layer IV in the somatosensory region (S I) of mouse cerebral cortex. *Brain Res.* 17, 205–242.